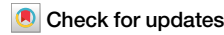


<https://doi.org/10.1038/s43247-024-01806-9>

A global overview of marine heatwaves in a changing climate



Antonietta Capotondi ^{1,2}✉, Regina R. Rodrigues ³, Alex Sen Gupta ^{4,5}, Jessica A. Benthuysen ⁶, Clara Deser ⁷, Thomas L. Frölicher ^{8,9}, Nicole S. Lovenduski ¹⁰, Dillon J. Amaya ², Natacha Le Grix ^{8,9}, Tongtong Xu ^{1,2}, Juliet Hermes ¹¹, Neil J. Holbrook ^{12,13}, Cristian Martinez-Villalobos ^{14,15}, Simona Masina ¹⁶, Mathew Koll Roxy ¹⁷, Amandine Schaeffer ^{18,19}, Robert W. Schlegel ²⁰, Kathryn E. Smith ²¹ & Chunzai Wang ^{22,23,24}

Marine heatwaves have profoundly impacted marine ecosystems over large areas of the world oceans, calling for improved understanding of their dynamics and predictability. Here, we critically review the recent substantial advances in this active area of research, including the exploration of the three-dimensional structure and evolution of these extremes, their drivers, their connection with other extremes in the ocean and over land, future projections, and assessment of their predictability and current prediction skill. To make progress on predicting and projecting marine heatwaves and their impacts, a more complete mechanistic understanding of these extremes over the full ocean depth and at the relevant spatial and temporal scales is needed, together with models that can realistically capture the leading mechanisms at those scales. Sustained observing systems, as well as measuring platforms that can be rapidly deployed, are essential to achieve comprehensive event characterizations while also chronicling the evolving nature of these extremes and their impacts in our changing climate.

In recent decades, episodes of warm ocean temperature extremes have been associated with more intense and frequent impacts on marine organisms, ecosystems and reliant human industries around the world^{1–3}. By analogy with their atmospheric counterpart, these extreme ocean temperature events have been termed “marine heatwaves” (MHWs)^{4,5}. Some of the most prominent events, together with the unprecedented warming during the boreal summer of 2023 are presented in Box 1. MHWs influence regional climate phenomena and often drive substantial impacts on the marine environment. For example, MHWs in the Indian Ocean have been found to modulate the monsoon winds and rains over the Indian subcontinent, impacting water and food security over the region⁶. MHWs interact with and intensify tropical cyclones, making them more destructive^{7–10}. Biological MHW impacts include mass mortality events in invertebrates, fish, birds and marine mammals^{1,11–13}, coral bleaching^{14,15}, declines in foundation species^{3,16,17} and entire ecosystem restructuring^{18,19}, with far-reaching socioeconomic impacts²⁰.

Recent reviews and perspectives^{13,21,22} have outlined major steps forward in understanding MHW characteristics, drivers, and predictability, along with the economic impacts they cause. However, in this rapidly evolving field, more recent research has provided new insights into MHWs, while generating important new questions and research avenues.

Although MHW research has primarily considered temperature extremes at the ocean surface, subsurface temperature extremes may be more intense and longer-lasting than their surface counterparts^{23–27}. Given the prevalence of life throughout the water column, subsurface MHWs need to be closely observed, mechanistically understood, and skillfully predicted. In addition, while the physical characterization of MHWs has mainly focused on large-scale events (Box 1), MHWs are now also studied in more localized coastal areas, marginal seas, and fjords^{28–31}, where they are negatively impacting the local ecology and coastal communities^{3,16}. MHWs are also increasingly being examined along with other extreme conditions, like high acidity or low-oxygen^{32,33}, sea level extremes³⁴, floods³⁵, droughts³⁶, severe weather events³⁷ or even terrestrial heat waves over the adjacent land³⁸. These “compound events” act as multiple stressors for marine life and societies.

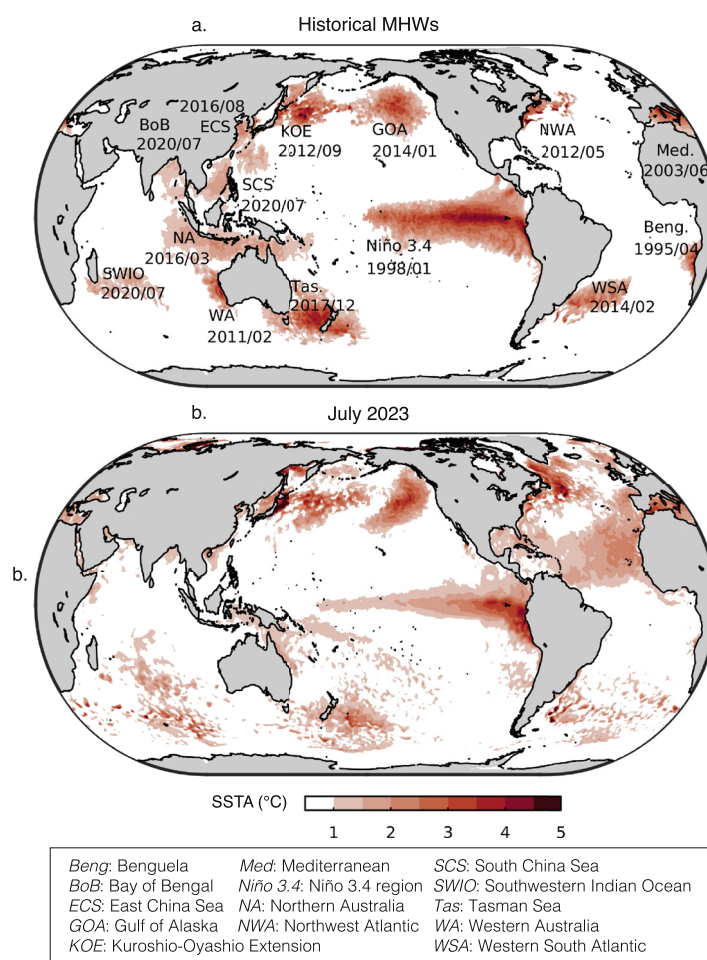
The ability to predict MHWs and compound events from days to seasons in advance is key for stakeholder preparation and mitigation efforts³⁹. Skillful forecasts require enhanced understanding of MHW drivers to assess their predictability, and prediction systems that realistically capture the processes underpinning that predictability^{21,40,41}. While progress has been made in prediction activities^{42,43}, additional improvements could be achieved through a deepened understanding of the relative roles of different

Box 1 | Historical marine heatwaves and the unprecedented summer of 2023

Recent decades have witnessed the occurrence of MHWs that were particularly intense, long-lasting and impactful (top panel of Box figure, showing SST anomalies above 1 °C at the peak month of each MHW). These most prominent MHWs generally occurred in different regions at different times. However, the boreal summer of 2023 recorded global monthly-mean SSTs at record high since the beginning of the instrumental record¹⁷⁸, with a large fraction of the ocean experiencing extreme conditions, as illustrated by the widespread SST anomalies⁷⁶ above the 90th percentile (1982–2011 baseline) during July 2023 (bottom panel of Box figure). In particular, average North Atlantic (0°–60°N, 0°–80°W) temperatures reached levels of warming that exceeded four standard deviations of the 1980–2011 period during parts of July and September 2023¹⁷⁹, with an annual average ~0.23 °C higher than in 2022¹⁸⁰.

What caused this unprecedented global extreme? The developing El Niño in 2023 can be expected to have caused an increase in radiative heating due to the influence of the El Niño SST pattern on atmospheric static stability and low-level clouds¹⁸¹. In addition, El Niño can alter the atmospheric circulation and cause the development of SST anomalies in different regions of the world, like the northeast Pacific¹¹⁰ and the tropical North Atlantic¹⁸², although warming in the tropical North Atlantic usually occurs after the peak of an El Niño event rather than during its development phase. The pattern of Atlantic warming is consistent with the negative phase of the North Atlantic Oscillation¹⁸³, which was indeed

strongly negative from mid-April to mid-May and most of July 2023. The concentration of the 2023 warming in near-surface waters¹⁸⁰ suggests that upper ocean stratification, possibly modulated by large-scale climate modes, may have played an important role in preventing the excess heat absorbed by the ocean from being effectively distributed downward, resulting in enhanced surface warming. Other hypotheses regarding the unprecedented 2023 warming include a decreased transport of Saharan dust to the western Atlantic, and a reduction of ship emissions following a 2020 international agreement, leading to an increase in radiative forcing¹⁸⁴, although the influence of these factors on Atlantic warming has yet to be demonstrated. Another proposed hypothesis pertains to the aftermath of the January 2022 Hunga Tonga-Hunga Ha'apai volcanic eruption in Tonga¹⁸⁵. This eruption emitted aerosols, which had cooling effects, while simultaneously releasing stratospheric water vapor, which had warming effects. However, these factors are estimated to explain, at most, a marginal net cooling of a few hundredths of a degree, rather than a warming¹⁸⁵. In addition to these mostly natural drivers, the ocean is estimated to have absorbed about 90% of the excess heat associated with global warming¹⁶¹, causing an average warming of the upper 2000m of the global ocean of ~6.6 10²¹ J/year over 1958–2023¹⁸⁰. Thus, it is very likely that climate change has contributed to the intensity and widespread coverage of the 2023 MHWs.



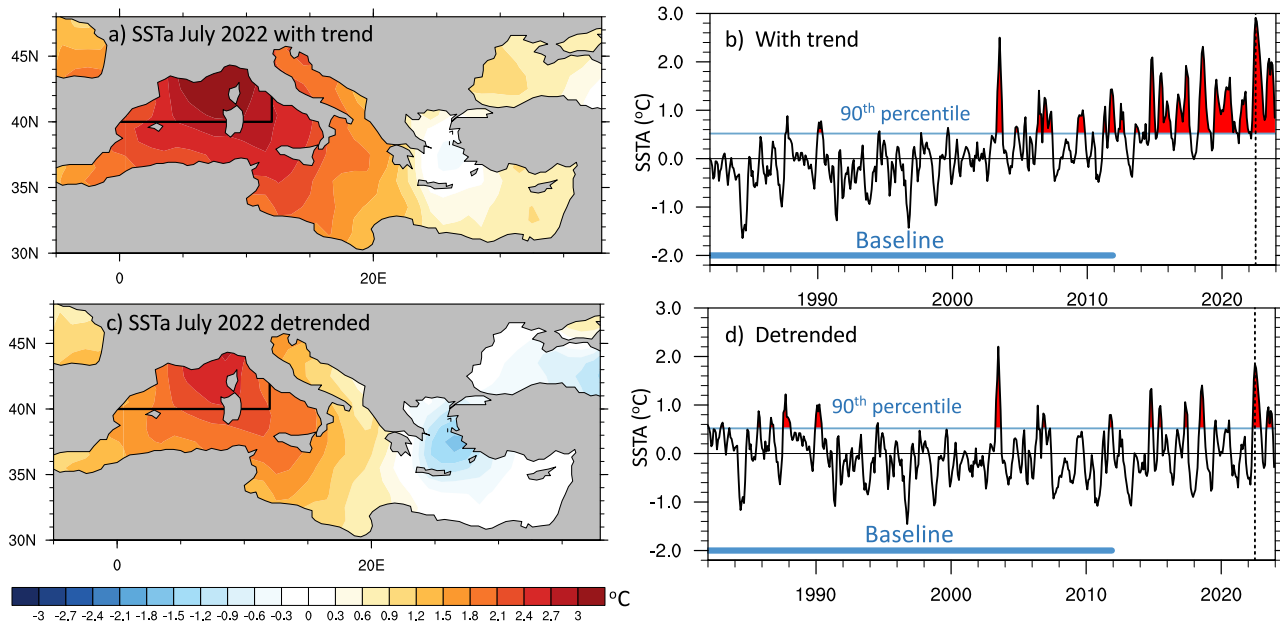


Fig. 1 | Influence of trends on marine heatwave definition. **a** SST anomaly (SSTA, °C) relative to the 1982–2011 climatology over the Mediterranean during July 2022 (dashed line in **b**) from NOAA-OISSTv2.1²⁶. Anomalies include the trend signal. **b** Monthly SST anomalies (seasonal cycle removed) averaged over the western Mediterranean (the region bounded by the black lines and the coast, i.e., north of 40°N, and west of 12°E). **c** As in (**a**), but with SST anomalies linearly detrended. **d** As in (**b**), but with anomalies linearly detrended. In (**b**) and (**d**), the thick blue horizontal line indicates the baseline period used to compute the climatology and to define the

90th percentile (thin horizontal blue lines), which for simplicity is chosen to be seasonally independent. In the presence of a trend, the western Mediterranean tends to be in a quasi-permanent MHW state toward the end of the record, while removal of the trend highlights isolated events since 2015, and also reveals more pronounced extreme events at the beginning of the record. The MHW in the boreal summer of 2003 emerges as an extremely intense event, irrespective of the presence of a trend signal.

MHW drivers, and dynamical model improvements, which include an assessment of the sensitivity of MHW forecasts to model resolution^{44–47}.

As the oceans continue to warm with anthropogenic climate change^{48,49}, defining MHWs under non-stationary conditions becomes increasingly challenging, as commonly used definitions will lead to a permanent MHW state in areas experiencing sufficient warming⁵⁰ (Fig. 1). In addition, separating the processes internal to the climate system from those of anthropogenic origin^{51,52} is key to the mechanistic understanding of the nature of MHWs and the assessment of their predictability and their future changes.

This article extends previous reviews^{13,21,22} by highlighting the new emerging areas in MHW research outlined above, including: a critical re-evaluation of MHW definitions and their detection, both at the surface and in the subsurface, in the presence of climate change; observational needs and new emerging “observing” strategies; advances in the understanding of both surface and subsurface MHW drivers to aid prediction efforts; compound events and their prediction; and investigations to assess future MHW projections using empirical approaches and state-of-the-art modeling systems. This review also provides a perspective on new and promising avenues for advancing our understanding and prediction capabilities of ocean extremes in the context of our changing climate.

Defining a marine heatwave

Defining a MHW involves multiple choices, each leading to outcomes with distinct implications. These choices may be motivated by the need to understand the physical drivers or impacts of a MHW, or they can be constrained by the characteristics of the available data, like record length or temporal resolution. For simplicity, MHWs have typically been analyzed using local definitions⁵³. However, since MHWs have a three-dimensional structure that evolves over time, other approaches are emerging^{25,54,55} to facilitate the tracking of extended surface or subsurface events over time.

Over the past decade, the majority of studies have adopted a common framework for defining MHWs. Following the widely used Hobday et al.⁵³

framework, a MHW occurs at a given location when daily sea surface temperature anomalies exceed the seasonally-varying 90th percentile climatology for five days or more (with dips below this threshold for two days or less ignored). The 90th percentile climatology is typically based on a fixed reference period, or “baseline”.

These threshold criteria were chosen in analogy with atmospheric heatwaves⁵⁶, and were not necessarily dictated by specific impacts in the marine environment. As such, other definitions have also been employed²², including, for example, definitions using the 99th percentile⁵⁷, approaches using monthly data^{41,42,51,52,58,59} instead of daily data (Fig. 1), annual maximum temperatures⁶⁰, or cumulative temperatures exceeding fixed thresholds, a criterion commonly used for coral bleaching monitoring and prediction^{61–63}. Attempts to incorporate information on biological impacts has led to the creation of MHW hazard indices, where species-tailored metrics were co-developed with stakeholders using absolute temperatures⁶⁴. With a fixed baseline, MHW conditions will become increasingly common as the ocean warms^{57,65}, potentially leading to a “permanent” MHW state in regions experiencing a high level of warming¹⁰ (Fig. 1). These changing characteristics may reflect the risk these events pose to some marine organisms, particularly those with slow adaptation rates¹³. However, considering a fixed baseline limits our ability to distinguish the slow climate change-related processes from the faster processes associated with internal modes of climate variability or synoptic weather conditions⁴⁰, with implications for understanding events’ predictability and assessing their prediction skill⁶⁶. Thus, there has been a recent call to remove the effects of mean warming when defining MHWs by detrending temperature time series⁶⁷ or using a shifting baseline period⁶⁸, especially for future projections. To define MHW characteristics, the decision to use a temperature threshold that remains fixed or changes over time will ultimately depend on the application being studied, the importance of maintaining consistency with past studies and the characteristics of the data record.

Given the availability of satellite-derived sea surface temperature (SST), many MHW studies have relied on daily gridded satellite data, starting in the

early 1980s. However, different datasets will have varying temporal and spatial resolutions, different interpolation accuracies, and may be sporadic and contain data gaps. Modified MHW definitions may be appropriate for different datasets and specific applications. For instance, monthly means can be used in regions characterized by long ocean memory (e.g., the tropical Pacific), or when the focus is on long-lasting MHWs^{20,69}. In all definitions, the temporal and spatial scales of the dynamics at play need to be considered.

Spatially, MHWs can cover large horizontal areas and extend deep into the water column. MHW structure is linked to their drivers and needs to be included in their characterization. While horizontal extent has been considered in studies assessing MHW projections^{57,70}, a number of new techniques have been developed to track connected MHW regions at the surface^{54,55,71} or in three-dimensional space^{25,72}, accounting for the splitting and merging of MHW regions. These techniques treat MHWs as objects that evolve in space and time providing an illustration of their areas of influence. Similar algorithms have also been applied to ocean acidification extremes in the Northeast Pacific⁷³, allowing an assessment of the severity of their impacts. To date, these tracking algorithms are purely statistical and do not incorporate information about event dynamics, but the use of tracking will provide new opportunities for understanding the extent of MHW systems as they evolve through time, and facilitate the identification of their underlying dynamics.

Observations for characterizing marine heatwaves

Observations are the foundation for characterizing and understanding MHWs. For more than a century, a diversity of ways to measure ocean temperature have been developed from in situ stationary and moving platforms (both passive and active) to remotely sensed methods (Box 2; Table 1 of Oliver et al.²²).

The challenge for observing MHWs is to measure ocean temperature at high temporal resolution and over a long period (decades) to define a threshold for extremes, while accounting for the inherent variability of temperature at different timescales. Advances in understanding MHWs globally have relied largely on satellite derived sea surface temperature products blended with near-surface in situ data provided from surface drifting buoys and ship underway systems (e.g., products such as the Operational SST and Ice Analysis (OSTIA) system^{74,75} and NOAA Daily Optimum Interpolation SST v2.1 dataset⁷⁶). On the other hand, long-term in situ temperature measurements from water samples and moorings have been crucial for characterizing temperature extremes at the daily timescale, although not representative of large areas. There are coastal locations distributed worldwide where ocean temperatures have been recorded since before the satellite era^{65,77–79}, providing insight into long-term trends of local ocean temperatures and changes in the frequency of temperature extremes. Only a few sites include sustained measurements extending through the water column, which have been crucial to understand subsurface MHW characteristics and drivers^{23,24,80}. Globally, the network of Argo floats has provided a transformative capability to study subsurface events by sampling ocean temperatures^{27,81} over the upper 2000 m for more than two decades⁸². However, using raw Argo profiles poses major analytical challenges, and Argo-derived gridded datasets are primarily available at monthly time resolution and lack coverage over continental shelves and marginal seas. Nevertheless, the combination of different observational platforms, for example, Argo and coastal moorings³⁹, is proving extremely valuable to achieve a comprehensive view of MHWs (Box 2).

To overcome issues associated with sparse and inconsistent observations, and extend analyses of MHWs back to the pre-satellite era, many studies have leveraged ocean reanalyses—models constrained by observations through data assimilation—to understand MHW drivers and dynamical processes^{41,83,84}, and analyze MHW characteristics at both the ocean surface and in the subsurface^{25,26}. Ocean reanalyses offer uniform data coverage in time and space, in some cases at high-resolution (e.g., GLORYS12v1⁸⁵), thus also facilitating the characterization of MHWs on continental shelves^{86,87}. Reanalysis products are subject to model errors and biases and may differ in their representation of MHWs over past decades⁸⁸.

Thus, they should be used with care to study extremes, especially in areas where limited observations were assimilated (e.g., the deep ocean or shelf regions). Some variables, like biogeochemical properties, are much less constrained by observations than physical quantities like temperature.

At longer timescales, a useful approach for increasing the sample size of extreme events is to use empirical models trained on observations, like Linear Inverse Models (LIMs⁸⁹), to produce multi-millennia synthetic time series. These synthetic data share similar statistical properties (covariances, autocorrelation, event evolution) with observations^{35,51,58} and allow exploration of the full range of possible MHW realizations that are consistent with the dynamics and noise structure of the training data.

Drivers of surface and subsurface marine heatwaves

The processes driving MHWs affect their characteristics, including duration, intensity and vertical structure, and are key for predicting their evolution. MHWs are driven by local heat fluxes associated with synoptic atmospheric conditions or ocean advective and mixing processes, and are sensitive to the ocean state (e.g., mixed layer depth). These local drivers may themselves be modulated by large-scale modes of climate variability or anthropogenic warming, and vary regionally and seasonally. In the extratropics, intense MHWs are commonly associated with persistent atmospheric highs, resulting in increased insolation and decreased wind speeds that reduce turbulent heat losses and vertical ocean mixing^{40,90–95}. Associated shallower mixed layers can further amplify the warming from surface heat fluxes^{59,83,96,97}. More broadly, heat budget analyses indicate that increased insolation and reduced evaporative cooling typically dominate the build-up of MHWs while decay is commonly driven by increased turbulent heat losses⁹⁸. In boundary current regions, anomalous warm oceanic advection is often important. Key examples include the 2011 Ningaloo Niño^{5,99,100} and the long-lived 2015/16 Tasman Sea MHW^{101,102}. Advection-driven MHWs typically have a smaller surface area, but last longer²¹ and may reach deeper¹⁰³ than atmospherically-driven events²¹. In the tropical Pacific, MHWs associated with El Niño Southern Oscillation (ENSO) are dynamically driven¹⁰⁴, with surface heat fluxes damping temperatures during both the onset and decay phases^{98,105}. In high-energy regions, like western boundary currents, oceanic mesoscale eddies and meanders, which often cross onto the shelf, can contribute to the onset, intensity, and longevity of MHWs at small temporal and spatial scales^{8,47,81,106}. Changes in atmosphere-ocean interactions, including positive cloud feedbacks (reduction of low-cloud cover leading to enhanced insolation) in response to the initial SST anomalies, may contribute to the maintenance and intensification of those anomalies, and increase their persistence, as documented for long-lasting events in the northeast Pacific^{107,108}.

Large-scale modes of climate variability can affect the likelihood of MHW occurrences regionally^{6,40}, by modulating the local drivers and the initial upper-ocean stratification. For example, the 2013/14 MHW in the southwest Atlantic was forced by atmospheric conditions associated with a wave train triggered by the Madden-Julian Oscillation in the tropical Indian Ocean³⁶. ENSO events are associated with a significant increase in the frequency, intensity and duration of MHWs across many parts of the global oceans^{65,90}, enhancing the forecast skill of MHWs and ocean acidity extremes^{42,109}, and influencing MHW projections⁵². For example, stronger equatorial Pacific easterly winds during La Niña events lead to an enhancement of the Indonesian Throughflow and Leeuwin Current, thereby transporting warm tropical waters to the Western Australian coast, creating favorable conditions for the development of MHWs⁹⁹. ENSO also affects the Northeast Pacific Ocean through both oceanic and atmospheric pathways¹¹⁰. However, ENSO's influence on MHWs may depend on the location of ENSO-related SST anomalies⁸⁴, and may be mediated by other modes of variability at interannual or decadal timescales^{40,41,94,111,112}. For example, a pre-existing positive Indian Ocean Dipole can increase the likelihood and predictability of MHWs off Western Australia up to 20 months in advance¹¹², while in the Northeast Pacific, MHW onset is influenced by low-frequency variability related to the Pacific Decadal Oscillation (PDO)^{41,111}. Interactions between tropical basins^{113,114} can also

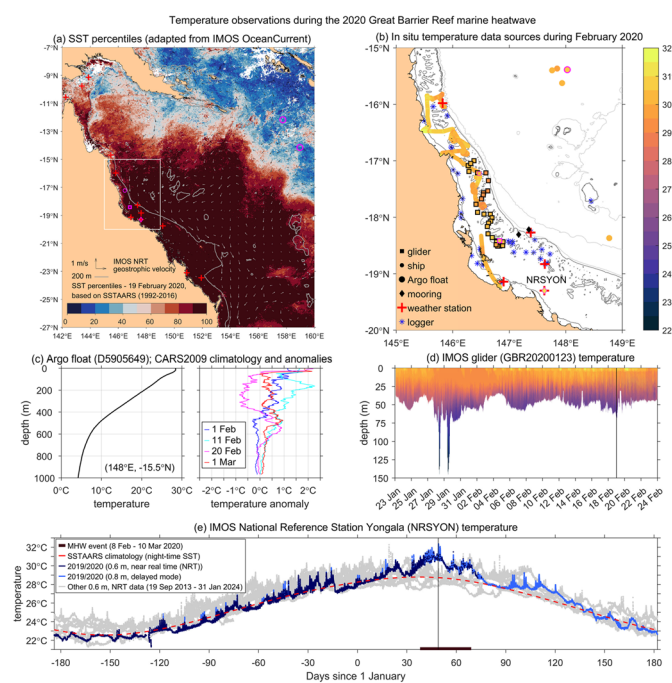
Box 2 | An integrated observing system for monitoring MHWs

Near real time ocean temperature observations and readily accessible visualizations of surface and subsurface conditions are critical for monitoring MHWs and to properly respond to the associated ecological risks. Gliders provide near real time data for a suite of oceanographic variables important for assessing MHW impacts on the marine environment. An example from Australia highlights how ocean gliders have been used to sample the water column during a MHW over several weeks, through Australia's Integrated Marine Observing System (IMOS) Event Based Sampling sub-facility (panel d of Box figure). In addition, combining different types of temperature observations relative to climatologies over the same reference period offers a comprehensive view of a temporally and spatially evolving MHW¹⁸⁶. We illustrate such a multi-platform system in the Box figure for the 2020 Great Barrier Reef MHW off northeast Australia.

Over the whole Great Barrier Reef, the MHW intensity peaked on 19 February 2020^{187,188}. On that day, extremely warm surface waters encompassed a wide extent of the Great Barrier Reef and Coral Sea, based on sea surface temperature (SST) percentiles obtained from the IMOS 6-day night-time multi-sensor L3S gridded SST^{189,190} relative to the 1992–2016 climatological distributions for that day of the year from the SST Atlas of Australian Regional Seas (SSTAARS¹⁹¹; panel a of the Box figure, also indicating the location of other near real time measuring platforms on that day). Several types of monitoring platforms collected temperature data during February 2020 over the region defined by the white box in panel a, as illustrated in panel b. The Australian Institute of Marine Science (AIMS) R/V Cape Ferguson measured near-surface water temperatures between 7 February 2020 (north) and 26 February 2020 (south)¹⁹² (small circles shaded with the temperature values, with a pink outline at 146.47°E, -17.23°N for 19 February 2020). These near-surface temperature measurements were complemented by those from Argo floats (larger circles in panel b, also shaded according to the temperature values), with a pink outline marking the position of one Argo float

(5905849) on 20 February 2020^{193,194}. This Argo float near -15.4°N, 147.9°E in the Coral Sea provided subsurface profiles (shown for the upper 1000 m in panel c of the Box figure). Based on the CARS2009 climatology¹⁹⁵, all profiles had warm anomalies near the surface, but the anomalies' vertical structure varied considerably at depth.

A glider (GBR2000123) was deployed through IMOS Event Based Sampling to monitor the MHW over the shelf¹⁹⁶. The glider traversed the continental shelf and slope from 23 January 2020 (north) to 24 February 2020 (south), as indicated by the colored (by temperature) track in panel b, measuring subsurface temperature (panel d, same colorbar as in panel b) and a suite of biophysical variables. The glider location on 19 February is indicated by the square with the pink outline (panel b). The glider measured relatively warm waters near the surface, while revealing cooler waters at depth through reef passages and over the continental slope. Finally, the IMOS National Reference Station Yongala (labeled NRSYON in panel b) provided near real time and delayed mode near-surface temperatures. These data are displayed in panel e of the Box figure relative to 1 January 2020, indicating a maximum near-surface temperature around February 19 (day 49, thin black vertical line), with anomalies exceeding +2 °C. These measurements during the MHW (marked by the horizontal line at the bottom of panel e), could be compared against the temperatures recorded at this station from 19 September 2013 to 31 January 2024^{197,198}, indicating the importance of sustained observations for detecting extremes. These datasets were complemented by in situ water temperature data collected from stationary sources (indicated in panel b) at other IMOS moorings, AIMS reef weather stations¹⁹⁹ and coral reef sites²⁰⁰. Together, these temperature measurements provided a comprehensive dataset for assessing the MHW's characteristics and impacts during the 2020 GBR mass coral bleaching event.



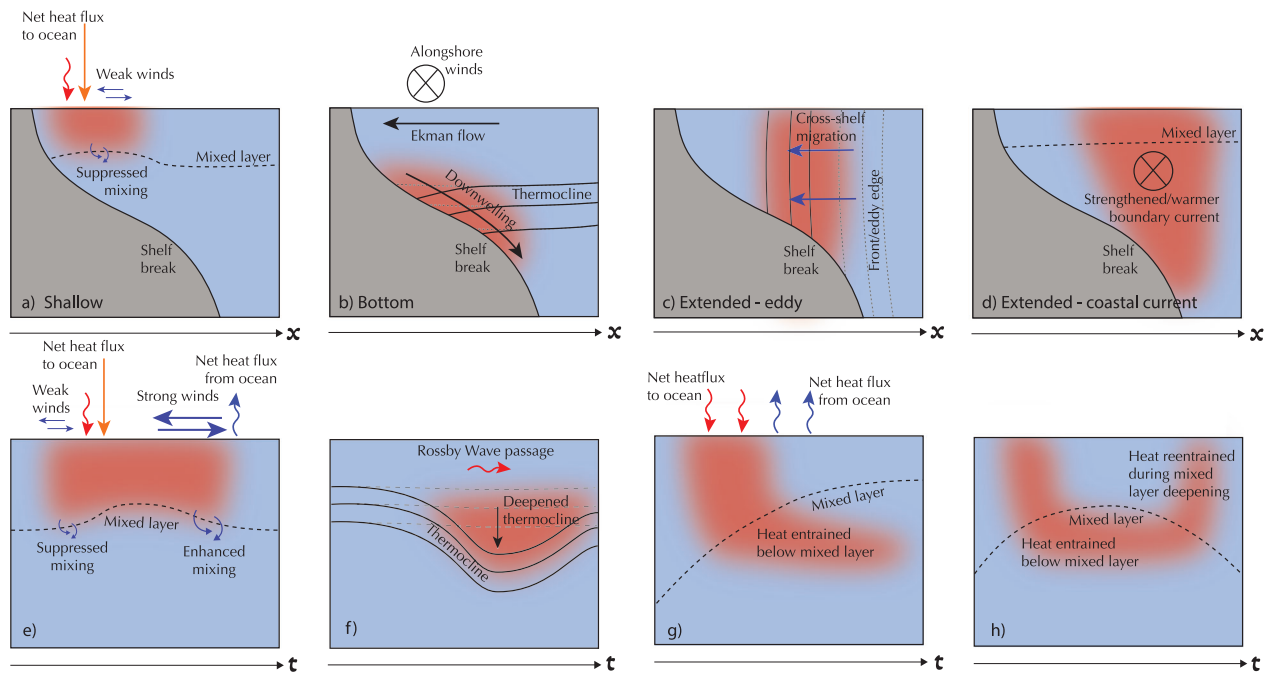


Fig. 2 | Vertical structures of MHWs. a-d Possible vertical structures of MHWs near the shelf, including: “shallow” MHWs which do not penetrate below the mixed layer (a); “Bottom” intensified events due to a downwelling thermocline near the bottom, resulting, for example, from alongshore winds, as illustrated for the Southern Hemisphere (b); “Extended” profiles from the surface to the bottom due to intrusion of warm eddies or western boundary meanders into the shelf (c) or due to warm alongshore advection (d). e-h Temporal evolution of subsurface MHWs

associated with: changes in upper-ocean mixing for shallow events (e); propagation of oceanic Rossby waves causing variations in thermocline depth (f); persistence of deep anomalies with no surface signature due to mixed layer shoaling (g); and re-emergence of deep anomalies at the surface when the mixed layer deepens (h). The subsurface structure of MHWs depends on the processes involved in their formation, as well as the region’s stratification and circulation.

contribute to MHW development, as exemplified by the 2020 MHWs in the Northwest Pacific and South China Sea^{115,116} and the unprecedented Northwest Pacific event of 2022¹¹⁷. Finally, MHWs in the far-eastern tropical Pacific (“coastal El Niño events”), result primarily from the constructive interference of the North and South Pacific Meridional Modes^{118,119}, and are not necessarily related to basin-wide ENSO conditions³⁵. Assessing the relative contributions and links between large-scale drivers is critical to fully understand and exploit the inherent system predictability and improve predictions¹²⁰.

MHWs extend into the subsurface ocean, with depth structures that may vary considerably depending on the region²⁷, the leading driving mechanisms and the local bathymetry, whether in open ocean or on the shelf. MHWs can be confined to the mixed layer (“shallow MHWs”), driven by enhanced air-sea heat fluxes, ocean advection or reduced wind-induced turbulent mixing (Fig. 2a, e), or they can penetrate well below the mixed layer²⁷. In shallow coastal regions, they can even extend to the ocean bottom (“Extended” events; Fig. 2c, d)^{24,86} due to the intrusion of warm eddies and western boundary current meanders onto the shelf (Fig. 2c) or through warm advection by alongshore currents (Fig. 2d), as shown by data from a near-shore mooring site in eastern Australia²⁴. Near the shelf, deep warm anomalies can result from downwelling processes and may coexist with surface cooling²⁴ (Fig. 2b). More generally, subsurface intensification through the dynamical movement of the thermocline may result from local Ekman pumping or from the passage of large-scale planetary waves (Fig. 2f), processes that occur ubiquitously throughout the ocean²⁶. These subsurface anomalies are often larger than surface anomalies, due to the movement of the strong vertical temperature gradients around the thermocline^{23,24,26,27,81,86,121}. As they evolve over time¹²¹ (Fig. 2e-h), subsurface MHWs can extend below the mixed layer during its seasonal shoaling and persist at depth even though the surface layer cools (Fig. 2g). They may sometimes be entrained back into a deepening mixed layer, and produce a delayed surface warming, a process known as “re-emergence”¹²² (Fig. 2h). Such evolutions were found in a simulation of the eastern tropical and North

Pacific¹²¹ and in Argo observations of Northeast Pacific MHWs during 2004–2020¹²³, and are likely to occur in other regions¹²⁴.

Compound and cascading events

Compound events are generally defined as a combination of extreme conditions and/or hazards that contribute to societal or environmental risk¹²⁵. As such, they stress both natural and human systems, causing socio-economic impacts such as loss of essential ecosystem services and income¹²⁵. Understanding their underlying physical processes is thus critical for predictability assessments. During a compound event, extreme conditions can occur simultaneously (e.g., high ocean temperatures and low oxygen concentrations in the ocean) or in close sequence, where one event can increase the system vulnerability to a successive event. For instance, droughts and heatwaves can lead to a higher risk of flash floods over land. Events can also occur concurrently over different regions with large-scale consequences, as exemplified by the widespread impacts on fisheries caused by MHWs and low upper ocean nutrient levels during El Niño events.

Marine heatwaves and terrestrial extremes

Our understanding is more advanced for extremes and compound events over land¹²⁶. However, work into ocean-land compound events is growing. For instance, atmospheric blocking over eastern South America and the western South Atlantic is associated with persistent high-pressure centers that can reduce cloud cover and latent heat loss, leading to simultaneous drought conditions over land and heatwaves in the adjacent ocean³⁶. Similarly, synoptic conditions driving terrestrial heatwaves in some locations around Australia are found to be conducive to the warming of the ocean, increasing the likelihood of a concurrent MHW³⁸. More generally, as many extreme extra-tropical MHWs are associated with persistent high-pressure centers⁹⁰, such systems, straddling the land and ocean, might plausibly lead to compound marine-terrestrial temperature extremes in coastal regions. MHWs can also be related to enhanced evaporation and transport of humidity, inducing heavy rainfall along coastal regions, such as

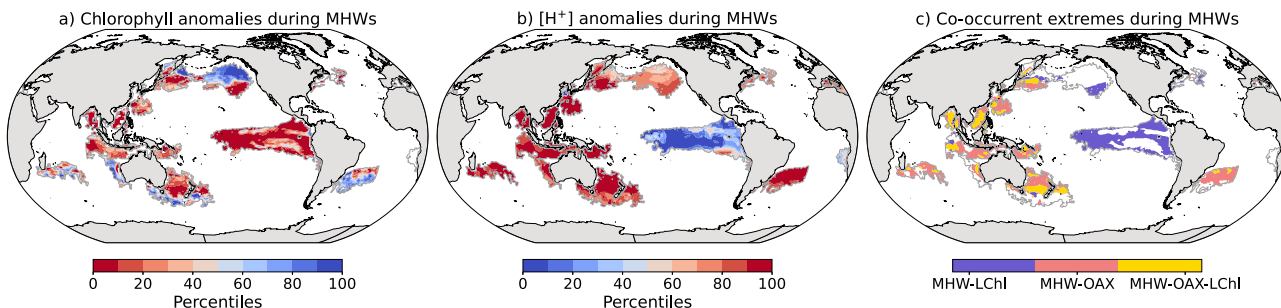


Fig. 3 | Near-surface biogeochemical anomalies and compound conditions during some impactful MHWs. The biogeochemical quantities are shown for the month and the area of the MHWs displayed in the top panel of Box 1's figure. The footprint of those MHWs is indicated by gray lines. **a** Percentile associated with the mean chlorophyll anomaly during the MHWs, compared to the local empirical distribution of chlorophyll monthly anomalies from 1998 to 2018. **b** Percentile associated with the mean $[H^+]$ anomaly during the MHWs, compared to the local empirical distribution of $[H^+]$ monthly anomalies from 1982 to 2019, based on observationally-derived data¹⁴³. **c** Extent of the MHWs co-occurring with a low

chlorophyll extreme event (MHW-LChl, in blue), a high acidity event (MHW-OAX, in red), and both (MHW-LChl-OAX, in yellow). LChl events are defined as events with chlorophyll anomaly percentiles on panel (a) lower than their 10th percentile, and OAX events as events with $[H^+]$ anomaly percentiles exceeding their 90th percentile. The chlorophyll data, corresponding to the mean chlorophyll concentration within the mixed layer, are obtained from the NASA Ocean Biogeochemical Model reconstruction¹⁷⁶, and are publicly available for 1998–2021 (<https://gmao.gsfc.nasa.gov/gmao/ftp/rousseau/Carlos/NOBM/>).

during the Tasman Sea MHW in 2015–16¹⁰¹ or the coastal MHW off Peru in 2017¹²⁷.

Marine heatwaves and ocean biogeochemical extremes

Given their potential impacts on marine organisms, there is growing interest in ocean biogeochemical extremes that can co-occur with temperature extremes (Fig. 3), including high acidity (OAX)^{73,128–131}, low oxygen (LOX)¹³² and low chlorophyll extremes (LChl)^{133,134}. These stressors may act additively or synergistically¹³⁵. For example, compound MHW-LOX events can have detrimental effects on aerobic metabolic rates, especially in ectotherms, i.e., cold-blooded organisms^{136–138}. Additionally, compound MHW-OAX events can adversely affect molluscs¹³⁹ or warm-water corals¹⁴⁰, while MHW-LChl events are often associated with extremely low fish biomass conditions¹⁴¹. Moreover, it is plausible that the concurrent extreme ocean acidity conditions amplified the devastating effects of the Northeast Pacific Marine Heatwave of 2014–2015¹⁴² (Box 1, top panel), also known as the “Blob”⁸³.

Compound MHW-OAX events are more likely to occur in the subtropics than in the equatorial Pacific and mid-to-high latitudes, as high temperatures in the subtropics strongly increase the hydrogen ion $[H^+]$ concentration (i.e., acidity)¹⁴³. At higher-latitudes, lower background temperatures limit this effect, while in the equatorial Pacific, reduced Dissolved Inorganic Carbon due to weaker upwelling leads to a decreased $[H^+]$ concentration, counteracting the effect of temperature. Conversely, hotspots of compound MHW-LChl events are found in the equatorial Pacific, along the boundaries of the subtropical gyres and in the northern Indian Ocean, often associated with El Niño events¹³³ and enhanced nutrient limitation on phytoplankton growth^{134,144}. Notably, the North Pacific MHW in 2014–2016 was identified as a quadruple compound event during some phases of its development, involving high temperature, low oxygen, high acidity and low chlorophyll levels^{32,133,145}. For example, in January 2014, the extreme warming of the Blob (Box 1, top panel) co-occurred with low chlorophyll over part of the MHW area (Fig. 3c).

Climate model projections indicate that long-term trends in acidification, deoxygenation, and nutrient decline in the low-latitude upper ocean will persist for decades^{146,147}, amplifying the frequency, intensity and scale of compound MHWs and biogeochemical extremes^{32,143}. Notably, even when using a shifting baseline, whereby the effect of long-term warming and OAX are removed, OAX events and compound MHW-OAX events are expected to increase due to projected increases in the seasonal and diurnal variations in $[H^+]$ ^{130,148,149}.

Despite initial studies, understanding ocean compound extreme events is still in its infancy³². A global perspective on the temporal and spatial characteristics of these events, especially at depth, and a mechanistic

understanding of relevant processes and their cascading impacts on ecosystems, are currently missing, mainly due to the lack of available subsurface data.

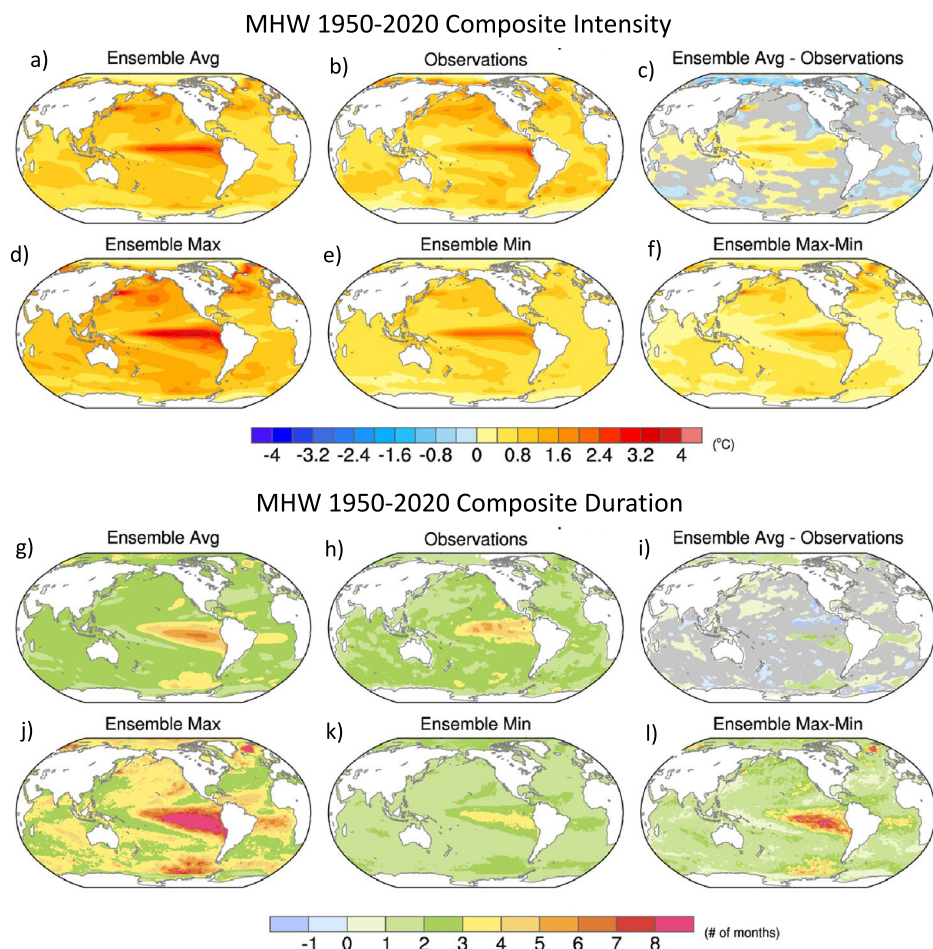
Climate models representation of marine heatwaves

Given the sparsity of long-term observational records, especially at depth, numerical models can help us to better understand MHW characteristics and their drivers. Global Earth system models (ESMs), which include both physical and biogeochemical components, are essential to provide future projections of both MHWs and biogeochemical extremes. But how well do climate models represent MHWs? Global coupled climate models vary in their degree of fidelity in representing climatological characteristics of basic MHW metrics (frequency, intensity and duration) at both daily^{44,60}, and monthly^{51,52} timescales. Generally, CMIP-type ESMs tend to overestimate the duration of MHWs^{47,52,150} (Fig. 4). In addition, regions of strong ocean currents are especially problematic in models without eddy-permitting resolution^{44,45,47}, due to the models’ inability to capture the influence of mesoscale eddies on MHW development in those regions¹⁰⁶. Observed changes in MHW characteristics over the historical period are also challenging for models to simulate, although those stemming from mean state changes are better represented than those due to changes in internal variability⁵¹. However, the observational record of surface MHWs is relatively short, consisting of approximately 40 years for daily SSTs derived from satellite remote sensing, and approximately 100 years for monthly SSTs measured by ships of opportunity, with subsurface MHW records being even shorter. Such observational records only provide a limited sample of all the possible realizations that are consistent with the dynamics and noise of the climate system.

Unlike observations, coupled climate models offer the potential for multiple realizations of the past and future, thereby enhancing sample sizes of extreme events. In particular, so-called “Single Model Initial-condition Large Ensembles” (SMILEs) have become a powerful tool in climate research for studying the simulated characteristics of internal variability and forced responses on local and regional scales¹⁵¹. SMILEs consist of many historical and future scenario simulations (generally 30–100) for a particular model, each starting from slightly different initial conditions, and allow a clean separation between the forced signal (the ensemble mean) and internal variability/extremes (departures from the ensemble mean). The power of SMILEs is only beginning to be exploited for the study of MHWs and their projected changes^{52,57,143,152}.

Figure 4 illustrates the effect of sampling uncertainty on MHW characteristics during the historical period 1950–2020, obtained from the 100-member CESM2 SMILE⁵², after the forced signal is removed. The composite MHW intensity (Fig. 4a) and duration (Fig. 4g) metrics based on all

Fig. 4 | Fidelity in climate models' representation of MHW statistics. **a–f** Composite MHW intensity ($^{\circ}\text{C}$) and **(g–l)** composite MHW duration (months) during 1950–2020 from the 100-member of the Community Earth System Model version 2 (CESM2) SMILE and observations (ERSSTv5)¹⁷⁵. **a, g** Ensemble average; **(b, h)** Observations; **(c, i)** Ensemble average minus Observations; **(d, j)** Ensemble maximum; **(e, k)** Ensemble minimum; **(f, l)** Ensemble maximum minus minimum. Gray shading in **(c, i)** indicates that observations lie within the 5th–95th percentile range of the CESM2 Large Ensemble. Adapted from Deser et al.⁵² © American Meteorological Society, used with permission.



ensemble members mask the considerable range found across individual realizations (Fig. 4d–f, j–l), underscoring the need for SMILEs to guard against sampling uncertainty. Since the single observational record (Fig. 4b, h) provides a limited sample size of extreme events, it may be challenging to separate true model biases from apparent biases stemming from inadequate sampling. One approach is to assess whether the characteristics of the single observed composite MHW lie outside the plausible (5th–95th percentile) range across SMILE members, in which case the model shows a likely bias (Fig. 4c, i). ESMs are also used for seasonal predictions of MHWs and other biogeochemical extremes. Thus, the fidelity of models in accurately simulating such extremes is critical for assessing the reliability of their predictions.

Prediction of marine heatwaves and associated biogeochemical extremes

Understanding MHW predictability and building effective prediction systems can greatly benefit marine management²¹. For example, accurate seasonal predictions of MHWs have the capacity to transform resource management practices that affect ecosystem services such as fisheries, aquaculture, and tourism^{21,43}. Motivated by many potential benefits, recent research has quantified subseasonal-to-seasonal MHW predictability and forecast skill using dynamical and statistical approaches^{41,42,153–155}.

Forecast systems based on global climate models have been used to estimate MHW probabilistic forecast skill and errors by comparing initialized hindcasts (i.e., retrospective forecasts) with the actual evolution of historical temperature anomalies. Results indicate that, for many open-ocean regions, these dynamical forecast systems are capable of skillfully predicting MHW onset, intensity, and duration several months in advance in both the surface and subsurface ocean^{42,153,154}. Forecast skill, quantified by

the correlation of ensemble-mean SST with that of the observations, is generally higher in the tropical and northeast extratropical Pacific, beating the skill associated with statistical (damped persistence) forecasts^{42,109,154}. MHW forecast skill is also higher in the subsurface (0–40 m) than the surface when compared to a reanalysis product, though subsurface skill outside the tropics is primarily due to persistence¹⁵³.

While in some cases dynamical forecast systems can produce skillful predictions of MHWs multiple months in advance, this is not always true. For example, 8.5-month lead forecasts initialized in July 1997 predicted an elevated likelihood of surface ocean MHW occurrence in the eastern Tropical Pacific, Gulf of Alaska, California Current, subtropical Atlantic and Indian Oceans, and the Pacific sector of the Southern Ocean during March 1998 (Fig. 5a). However, dynamical 8.5-month lead forecasts initialized in March 2013 predicted low probability of surface ocean MHWs nearly everywhere in the global ocean for November 2013 (Fig. 5b). The observed SST anomalies in March 1998 (Fig. 5c) and November 2013 (Fig. 5d) indicate that the forecasts generated in July 1997 were more accurate than the March 2013 forecasts. The accuracy of the July 1997 initialized forecast is primarily due to the development of the 1997/1998 El Niño event, as ENSO predictability imparts prediction skill to initialized forecasts of MHWs^{21,42}. The March 2013 initialized forecast provides little indication of the development of the Blob in late-2013^{33,156}. This comparison highlights the difficulties in forecasting MHWs that are driven by stochastic atmospheric processes, like the Blob¹⁵⁵, or energized by modes of variability not accurately captured by the models. On the other hand, surface and subsurface MHWs that are associated with ENSO variability and/or oceanic teleconnections may be predictable several months in advance^{21,42,109,153}.

Statistical MHW forecasts may have similar skill as forecasts from dynamical models, while requiring substantially less computational

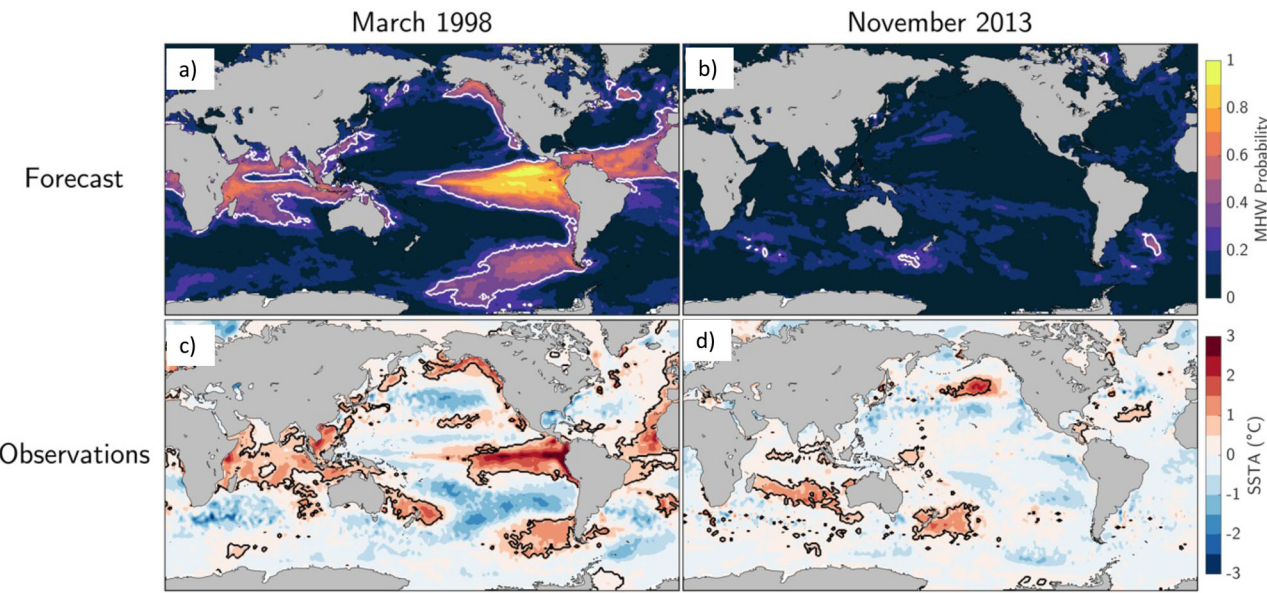


Fig. 5 | Dependence of MHW forecast skill on El Niño. Forecasted MHW probabilities for two periods: (a) March 1998, and (b) November 2013, based on probabilistic forecasts of linearly detrended anomalies from the North American Multimodel Ensemble¹⁷⁷ initialized 8.5 months prior (i.e., July 1997 and March 2013,

respectively). White contour indicates 30% probability of occurring MHW conditions. c–d Observed monthly SST anomalies (°C) for the two forecasted periods. Black contours indicate observed MHW conditions.

resources. McAdam et al.¹⁵³ showed that a simple statistical persistence forecast can skillfully predict the number of subsurface MHW days one season in advance in approximately half of the ocean, but it underestimates the number of events compared to the reanalysis product used as validation. More complex statistical models, including empirical-dynamical models such as Linear Inverse Models (LIMs), can be used to probe sources of predictive skill for particular regions or events. For example, LIM-based studies showed that a decadal mode of variability was a precursor for MHW growth in the Northeast Pacific Blob region⁴¹, and that predictability of MHWs off Western Australia was enhanced up to 20 months in advance by the presence of a positive Indian Ocean Dipole¹⁵⁷.

ESM dynamical forecast systems display promising levels of forecast skill for surface and subsurface biogeochemical properties affected by MHWs, such as oxygen, acidity, or productivity^{158–160}. Recent studies have explored dynamical forecast skill of ocean biogeochemical extremes. For example, Mogen et al.¹⁰⁹ showed that a coupled model produces skillful forecasts of OAX events associated with aragonite saturation state anomalies, at lead times of up to twelve months in some regions, and further identify ENSO events as playing a key role in predicting this type of extremes. Such findings inspire efforts to include biogeochemical predictions in operational forecasting systems for MHWs.

Marine heatwaves in a changing climate

The ocean has stored more than 90% of the excess heat¹⁶¹ that has accumulated in the Earth System due to human-induced increases in radiative forcing agents, resulting in ocean warming that is projected by climate models to become large and widespread by the end of the century (Fig. 6a). Such slow background warming exacerbates naturally-occurring temperature excursions, resulting in increased frequency, intensity and duration of extreme SST events. Indeed, attribution studies have shown that the majority of the most impactful MHWs worldwide over recent decades could not have occurred without the influence of global warming^{50,57,70}. In the presence of the global warming trend, climate models project large increases in the frequency, intensity, duration and spatial extent of warm temperature extremes, with the magnitude of the increase becoming progressively larger at higher warming levels⁵⁷.

In addition to the long-term ocean warming trend, climate change can also affect ocean extremes through changes in variability. An increase in

mean SSTs, relative to, for example, pre-industrial levels or early historical periods, will result in a shift of the probability density function (PDF) toward larger values, enhancing the likelihood of more severe events (Fig. 6c–e). Changes in variability, however, alter the PDF's width, which can also affect the probability of SST extremes (Fig. 6c–e). Moreover, changes in internal SST variability may be asymmetric, and lead to increased probabilities for either warm or cold extremes (Fig. 6d). The relative influence of the warming trend vs. anthropogenically-induced changes in internal variability on MHW statistics varies geographically^{51,52}, with the long-term warming trend often accounting for more than 90% of the total changes^{46,50–52,57,143,162}, as illustrated for CESM2 in Fig. 6b. Exceptions are the Arctic, where internal variability can account for 30–40% of MHW intensity changes, and the Northeast Atlantic, with values up to 80% (Fig. 6b). While separating the effects of the temperature trend and internal variability on MHW characteristics is critical for the mechanistic understanding of MHWs, and for assessing events' predictability, this separation is challenging. The climate change trend may be nonlinear^{51,79}, and failure to accurately account for such nonlinearity may result in an apparent change in internal variability⁵¹. Approaches used to estimate the forced trend in observations for MHW studies include the use of univariate⁵⁰ or multivariate^{51,163,164} statistical approaches, while large ensembles can be used in the modeling context.

There are several ways by which anthropogenic forcing can alter internal climate variability. Mixed layer shoaling may occur with global warming^{97,152}, resulting in increased mixed-layer temperatures for the same level of atmosphere-to-ocean heat exchange. The projected increase in upper-ocean stratification¹⁶⁵ and ocean heat content¹⁶² can alter the characteristics of key large-scale drivers of MHWs. For example, increased stratification in the equatorial Pacific has been related to future enhancements of ENSO amplitude in several climate models¹⁶⁶, while in the extratropics, stronger stratification will result in faster oceanic Rossby waves and shorter adjustment processes, potentially leading to reduced growth and predictability of decadal modes of variability like the PDO¹⁶⁷. In addition, changes in extra-tropical atmospheric circulation variability driven by mean state changes and by teleconnections from changing ENSO behavior, could alter MHW characteristics through impacts on air-sea heat and momentum exchange¹⁶⁸. Dramatic changes in Arctic sea-ice coverage and amplified Arctic warming may have been responsible for the changes in atmospheric

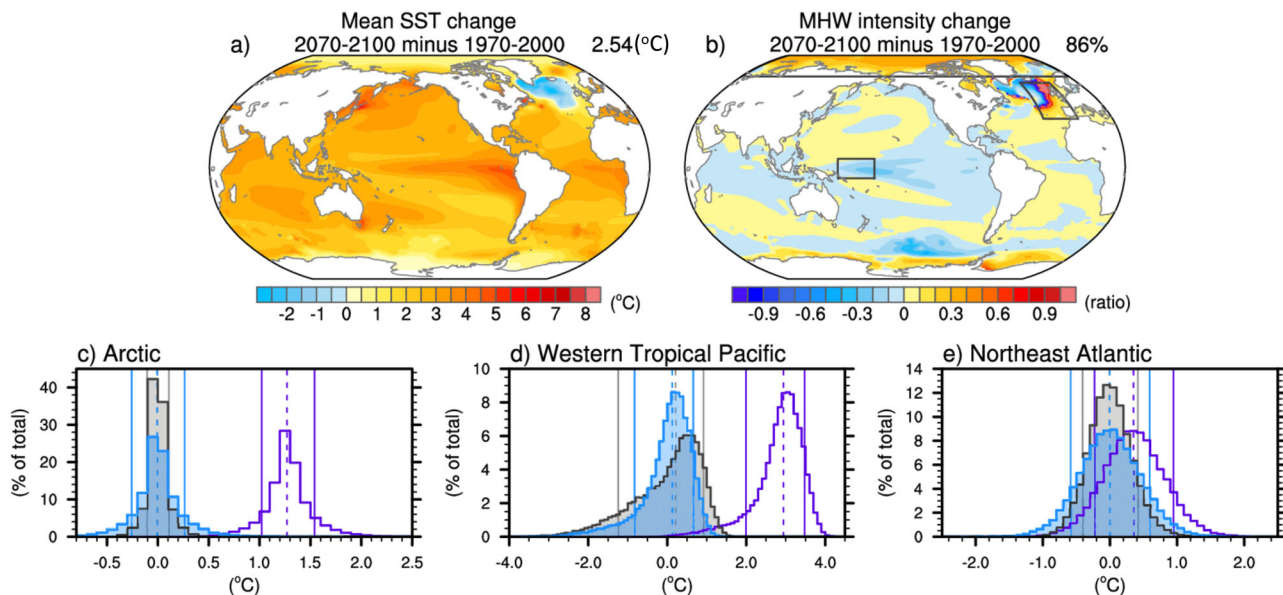


Fig. 6 | Projected changes in MHWs in one climate model Large Ensemble.

a Changes in mean SST (2070–2100 minus 1970–2000) based on the ensemble mean of the CESM2 large ensemble according to the SSP370 scenario. **b** Changes in composite MHW intensity (2070–2100 minus 1970–2000) due to internal variability divided by the intensity changes due to both changes in variability-plus-mean state. **c–e** Histograms of area-averaged SST (°C) from the CESM2 large ensemble for **(c)** Arctic (poleward of 67°N), **(d)** western tropical Pacific (8°S–6°N, 155°E–175°W), and **(e)** northeast Atlantic (35°–62°N, 30°–0°W) based on all months from all 100 ensemble members during 1970–2000 (gray) and 2070–2100 (blue) after removing

the ensemble-mean climatological seasonal cycle for each period. The regions considered for computing the histograms are shown by the boxes in **(b)**. Purple histograms are the same as the blue histograms but with the mean state change (2070–2100 minus 1970–2000) added back in. The 10th and 90th percentiles of each distribution are shown as vertical solid lines, and the 50th percentile is shown as a vertical dashed line. The number in the upper right of **(a)** indicates the global mean ocean temperature difference (°C), while the number in the upper right of **(b)** indicates the fractional area (%) of values in the range –0.1 and +0.1. Adapted from Deser et al.⁵² © American Meteorological Society, used with permission.

circulation and Northeast Pacific surface heat fluxes that led to the unprecedented MHWs in that region in recent decades¹⁶⁹. The reduction in sea-ice will also result in an increase in MHW activity near the marginal ice zone^{52,124}.

Changes in ENSO characteristics are particularly critical for future MHWs. Consistent with the observed association between El Niño events and the enhanced likelihood of MHW occurrence^{40,65}, multi-model large ensembles project a significant reduction in MHW areal coverage, intensity and duration during ENSO-neutral periods relative to all periods, when the mean warming component is removed⁵². Thus, changes in ENSO variability might significantly influence the statistics of MHWs in the future, highlighting the critical need of constraining the spread in expected ENSO changes¹⁷⁰, and achieving more reliable future projections.

Summary and future perspectives

MHWs are an active and fast evolving area of research, and significant progress has been made in the last few years. Definitions of MHWs have been critically re-evaluated to best characterize these events and their drivers in the presence of the climate change trend, and approaches have been developed that incorporate spatial dimensions and time evolution^{25,54,55}. On the observational side, multi-platform systems capable of providing the three-dimensional structure of MHWs in near real-time are now emerging (Box 2). Additional advances include a deepened understanding of local and remote drivers of MHWs^{41,112,120,171,172}, explorations of subsurface MHWs and their possible structures, investigations of land-ocean and physical-biogeochemical compound events, future projections of MHWs and related uncertainty⁵², and evolving efforts in MHW prediction^{42,109,153,154}. Yet, to achieve a more robust assessment of MHW predictability, additional investigations are needed to better understand large-scale drivers of MHWs in different regions and during different seasons, and their interplay in altering local processes responsible for MHW growth, evolution and persistence. MHW definitions should also be extended to reflect MHW mechanisms, and allow event characterization based on their primary drivers.

A key question for MHW prediction and projection, is whether climate models currently used for seasonal predictions and for future projections can realistically simulate MHW mechanisms beyond basic, local surface statistics (like frequency, intensity and duration). For example, can models simulate events similar to the most prominent and impactful MHWs in the historical record? Are these events driven by the same local and remote influences as in nature? Do they have similar subsurface characteristics? Assessing models' fidelity in simulating modes of variability that can influence MHW development is also critical. Given the strong association between ENSO events and MHW occurrences^{40,65,90}, the reliability of simulated MHWs in both present and future scenarios strongly depend on the models' ability to realistically simulate ENSO. However, ENSO representation in climate models still shows significant biases, and its future projections vary significantly across models¹⁷⁰, calling for an in-depth understanding of model differences and biases, and concerted efforts toward model improvement.

In order to provide forecasts that are useful for stakeholders, greater focus is needed on higher resolution global and regional models, that are able to resolve processes occurring on the shelf or at scales relevant for coastal topography (e.g., embayments, fjords, coral atolls, etc.). Regional models, which are currently under development for some regions¹⁷³, should include biogeochemistry, and be used for prediction and projection applications. The availability of observations at these scales is also critical for model development and validation.

While many studies have discussed MHW impacts, this area of research is still evolving. For example, some long-lasting MHW impacts are just emerging, like the decline of the humpback whales in the North Pacific since 2014, attributed to loss of prey after the 2014–16 MHW¹⁷⁴. Conversely, other research suggests that MHWs are not a dominant driver of change in demersal fishes over the recent decades⁸⁷. Aspects in need of further research include: (1) influence of MHWs on local atmospheric extremes, like atmospheric rivers and heatwaves; (2) connections between temperature extremes and oceanic biogeochemical extremes^{32,133}; and (3) long-term and cumulative consequences of MHWs on marine life across trophic levels, as

well as assessment of recovery times in different regions. Also, given the reported impact of MHWs on air-sea CO₂ fluxes⁶⁹ and their documented association with cloud feedback in some regions^{107,108}, a deeper exploration of possible MHW influences on the Earth's carbon and radiation budgets may be important.

Observations of physical, biogeochemical and ecological quantities, at the surface and especially in the ocean subsurface, are key to all of the above aspects of MHW research. Given that MHWs can occur anytime, anywhere, concerted efforts to improve our global capacity to observe the state of the ocean both at the surface and in the subsurface are needed to properly monitor MHWs and their cascading impacts, as well as to constrain ocean reanalyses and assess model performance. Sustained observations, both globally (e.g., satellite, (deep-) Argo) or regionally (e.g., moorings), in conjunction with ocean reanalyses and long time series from empirical models, are necessary to examine long-term changes in ocean properties and robustly assess the statistics of extreme warm events relative to those long-term changes. On the other hand, systems that can be rapidly deployed for real-time monitoring (Box 2), provide not only a comprehensive characterization of individual events, but also immediate guidance to decision-makers. Such multi-platform systems, however, may not be feasible everywhere. Assessing which observations can most effectively monitor MHWs in different regions is a critical issue that the MHW community must address.

Enhanced understanding of MHWs and their impacts is essential to guide and support adaptation and mitigation strategies. The tremendous level of ecological, economical and societal losses resulting from these ocean extremes calls for urgent actions to drastically reduce greenhouse gas emissions in order to limit the devastating consequences of climate change.

Data availability

The data used in this review are properly cited in the relevant sections. The NOAA OISSTv2.1⁷⁶ data were obtained from NOAA/OAR/PSL, Boulder, Colorado, USA, via their website at <https://psl.noaa.gov/>. The ERSSTv5¹⁷⁵ dataset is publicly available from www.ncei.noaa.gov/products/extended-reconstructed-sst. Argo data are freely available from <https://argo.ucsd.edu> and <https://www.ocean-ops.org>. IMOS data were obtained from the Australian Ocean Data Network Portal: <https://portal.aodn.org.au/>. Chlorophyll data were obtained from the NASA Ocean Biogeochemical Model reconstruction¹⁷⁶, and are publicly available for 1998–2021 from <https://gmao.gsfc.nasa.gov/gmaoftp/rousseaux/Carlos/NOBM/>. Global climate forecasts from the NMME¹⁷⁷ can be obtained from the IRI/LDEO climate data library (<https://iridl.ldeo.columbia.edu/SOURCES/Models/.NMME/>). The CESM2 model output used to produce Figs. 4 and 6 are publicly available from <https://www.cesm.ucar.edu/community-projects/mmlea> and <https://esgf-node.llnl.gov/search/cmip6/>.

Received: 5 June 2024; Accepted: 17 October 2024;

Published online: 20 November 2024

References

1. Smith, K. E. et al. Socioeconomic impacts of marine heatwaves: global issues and opportunities. *Science* **374**, eabj3593 (2021).
2. Frölicher, T. L. & Laufkötter, C. Emerging risks from marine heat waves. *Nat. Commun.* **9**, 650 (2018).
3. Smith, K. E. et al. Global impacts of marine heatwaves on shallow coastal foundation species. *Nat. Commun.* **15**, 5052 (2024).
4. Pearce, A. et al. The “marine heat wave” off Western Australia during the summer of 2010/11. Fisheries Research Report No. 222. Department of Fisheries, Western Australia. 40pp.
5. Pearce, A. F. & Feng, M. The rise and fall of the “marine heat wave” off Western Australia during the summer of 2010/2011. *J. Mar. Syst.* **111-112**, 139–156 (2013).
6. Saranya, J. S., Roxy, M. K., Dasgupta, P. & Anand, A. Genesis and trends in marine heatwaves over the Tropical Indian Ocean and their interaction with the Indian summer monsoon. *J. Geophys. Res. Oceans* **127**, e2021JC017427 (2022).
7. Singh, V. K., Roxy, M. K. & Deshpande, M. Role of warm ocean conditions and the MJO in the genesis and intensification of extremely severe cyclone Fani. *Sci. Rep.* **11**, 3607 (2021).
8. Mawren, D., Hermes, J. & Reason, C. J. C. Marine heat waves and tropical cyclones—two devastating types of coastal hazard in South-eastern Africa. *Estuar. Coast. Shelf Sci.* **277**, 108056 (2022).
9. Rathore, S. et al. Interactions between a marine heatwave and tropical cyclone Amphan in the Bay of Bengal in 2020. *Front. Clim.* **4** <https://doi.org/10.3389/fclim.2022.861477> (2022).
10. Roxy, M. K. et al. in *The Indian Ocean and its Role in the Global Climate System* (eds Caroline C. U. & R. R. Hood) 469–482 (Elsevier, 2024).
11. Jones, T. et al. Massive Mortality of a Planktivorous seabird in response to a marine heatwave. *Geophys. Res. Lett.* **45**, 3193–3202 (2018).
12. Garrabou, J. et al. Marine heatwaves drive recurrent mass mortalities in the Mediterranean Sea. *Glob. Change Biol.* **28**, 5708–5725 (2022).
13. Smith, K. E. et al. Biological impacts of marine heatwaves. *Annu. Rev. Mar. Sci.* **15**, 119–145 (2023).
14. Eakin, C. M., Sweatman, H. P. A. & Brainard, R. E. The 2014–2017 global-scale coral bleaching event: insights and impacts. *Coral Reefs* <https://doi.org/10.1007/s00338-019-01844-2> (2019).
15. Moriarty, T., Leggat, W., Heron, S. F., Steinberg, R. & Ainsworth, T. D. Bleaching, mortality and lengthy recovery on the coral reefs of Lord Howe Island. The 2019 marine heatwave suggests an uncertain future for high-latitude ecosystems. *PLOS Clim.* **2**, e0000080 (2023).
16. Filbee-Dexter, K. et al. Marine heatwaves and the collapse of marginal North Atlantic kelp forests. *Sci. Rep.* **10**, 13388 (2020).
17. Smale, D. A. et al. Marine heatwaves threaten global biodiversity and the provision of ecosystem services. *Nat. Clim. Change* **9**, 306–312 (2019).
18. Wernberg, T. et al. An extreme climatic event alters marine ecosystem structure in a global biodiversity hotspot. *Nat. Clim. Change* **3**, 78–82 (2013).
19. Stuart-Smith, R. D., Brown, C. J., Ceccarelli, D. M. & Edgar, G. J. Ecosystem restructuring along the Great Barrier Reef following mass coral bleaching. *Nature* **560**, 92–96 (2018).
20. Cheung, W. W. L. et al. Marine high temperature extremes amplify the impacts of climate change on fish and fisheries. *Sci. Adv.* **7**, eabh0895 (2021).
21. Holbrook, N. J. et al. Keeping pace with marine heatwaves. *Nat. Rev. Earth Environ.* **1**, 482–493 (2020).
22. Oliver, E. C. J. et al. Marine heatwaves. *Annu. Rev. Mar. Sci.* **13**, 313–342 (2021).
23. Schaeffer, A. & Roughan, M. Subsurface intensification of marine heatwaves off southeastern Australia: the role of stratification and local winds. *Geophys. Res. Lett.* **44**, 5025–5033 (2017).
24. Schaeffer, A., Sen Gupta, A. & Roughan, M. Seasonal stratification and complex local dynamics control the sub-surface structure of marine heatwaves in Eastern Australian coastal waters. *Commun. Earth Environ.* **4**, 304 (2023).
25. Sun, D., Li, F., Jing, Z., Hu, S. & Zhang, B. Frequent marine heatwaves hidden below the surface of the global ocean. *Nat. Geosci.* **16**, 1099–1104 (2023).
26. Fragkopoulou, E. et al. Marine biodiversity exposed to prolonged and intense subsurface heatwaves. *Nat. Clim. Change* **13**, 1114–1121 (2023).
27. Zhang, Y., Du, Y., Feng, M. & Hobday, A. J. Vertical structures of marine heatwaves. *Nat. Commun.* **14**, 6483 (2023).
28. Reed, D. et al. Extreme warming challenges sentinel status of kelp forests as indicators of climate change. *Nat. Commun.* **7**, 13757 (2016).

29. Jackson, J. M., Johnson, G. C., Dosser, H. V. & Ross, T. Warming from recent marine heatwave lingers in deep British Columbia fjord. *Geophys. Res. Lett.* **45**, 9757–9764 (2018).

30. Yao, Y. & Wang, C. Variations in summer marine heatwaves in the South China Sea. *J. Geophys. Res. Oceans* **126**, e2021JC017792 (2021).

31. Koehlinger, J. A., Newton, J., Mickett, J., Thompson, L. & Klinger, T. Large and transient positive temperature anomalies in Washington's coastal nearshore waters during the 2013–2015 northeast Pacific marine heatwave. *PLoS One* **18**, e0280646 (2023).

32. Gruber, N., Boyd, P. W., Frölicher, T. L. & Vogt, M. Biogeochemical extremes and compound events in the ocean. *Nature* **600**, 395–407 (2021).

33. Hauri, C. et al. More than marine heatwaves: a new regime of heat, acidity, and low oxygen compound extreme events in the Gulf of Alaska. *AGU Adv.* **5**, e2023AV001039 (2024).

34. Han, W. et al. Sea level extremes and compounding marine heatwaves in coastal Indonesia. *Nat. Commun.* **13**, 6410 (2022).

35. Martinez-Villalobos, C., Dewitte, B., Garreaud, R. G. & Loyola, L. Extreme coastal El Niño events are tightly linked to the development of the Pacific Meridional Modes. *npj Clim. Atmos. Sci.* **7**, 123 (2024).

36. Rodrigues, R. R., Taschetto, A. S., Sen Gupta, A. & Foltz, G. R. Common cause for severe droughts in South America and marine heatwaves in the South Atlantic. *Nat. Geosci.* **12**, 620–626 (2019).

37. Dzwonkowski, B. et al. Compounding impact of severe weather events fuels marine heatwave in the coastal ocean. *Nat. Commun.* **11**, 4623 (2020).

38. Pathmeswaran, C., Sen Gupta, A., Perkins-Kirkpatrick, S. E. & Hart, M. A. Exploring potential links between co-occurring coastal terrestrial and marine heatwaves in Australia. *Front. Clim.* **4** <https://doi.org/10.3389/fclim.2022.792730> (2022).

39. Hobday, A. J. et al. With the arrival of El Niño, prepare for stronger marine heatwaves. *Nature* **621**, 38–41 (2023).

40. Holbrook, N. J. et al. A global assessment of marine heatwaves and their drivers. *Nat. Commun.* **10**, 2624 (2019).

41. Capotondi, A., Newman, M., Xu, T. & Di Lorenzo, E. An optimal precursor of Northeast Pacific marine heatwaves and central Pacific El Niño events. *Geophys. Res. Lett.* **49**, e2021GL097350 (2022).

42. Jacox, M. G. et al. Global seasonal forecasts of marine heatwaves. *Nature* **604**, 486–490 (2022).

43. Hartog, J. R., Spillman, C. M., Smith, G. & Hobday, A. J. Forecasts of marine heatwaves for marine industries: reducing risk, building resilience and enhancing management responses. *Deep Sea Res. Part II Top. Stud. Oceanogr.* **209**, 105276 (2023).

44. Pilo, G. S., Holbrook, N. J., Kiss, A. E. & Hogg, A. M. Sensitivity of marine heatwave metrics to ocean model resolution. *Geophys. Res. Lett.* **46**, 14604–14612 (2019).

45. Hayashida, H., Matear, R. J., Strutton, P. G. & Zhang, X. Insights into projected changes in marine heatwaves from a high-resolution ocean circulation model. *Nat. Commun.* **11**, 4352 (2020).

46. Guo, X. et al. Threat by marine heatwaves to adaptive large marine ecosystems in an eddy-resolving model. *Nat. Clim. Change* **12**, 179–186 (2022).

47. Bian, C. et al. Oceanic mesoscale eddies as crucial drivers of global marine heatwaves. *Nat. Commun.* **14**, 2970 (2023).

48. Collins, M. et al. in *IPCC Special Report on the Ocean and Cryosphere in a Changing Climate* (eds H.-O. Portner et al.) Ch. Extremes, Abrupt Changes and Managing Risk, pp. 589–655 (Cambridge University Press, 2019).

49. Fox-Kemper, B. et al. in *Climate Change 2021: The Physical Science Basis. Contribution of Working Group I to the Sixth Assessment Report of the Intergovernmental Panel on Climate Change* (eds V. Masson-Delmotte et al.) Ch. Ocean, Cryosphere and Sea Level Change., pp. 1211–1362 (Cambridge University Press, 2021).

50. Oliver, E. C. J. et al. Projected marine heatwaves in the 21st century and the potential for ecological impact. *Front. Marine Sci.* **6** <https://doi.org/10.3389/fmars.2019.00734> (2019).

51. Xu, T. et al. An increase in marine heatwaves without significant changes in surface ocean temperature variability. *Nat. Commun.* **13**, 7396 (2022).

52. Deser, C. et al. Future changes in the intensity and duration of marine heat and cold waves: insights from coupled model initial-condition large ensembles. *J. Clim.* **37**, 1877–1902 (2024).

53. Hobday, A. J. et al. A hierarchical approach to defining marine heatwaves. *Prog. Oceanogr.* **141**, 227–238 (2016).

54. Sun, D., Jing, Z., Li, F. & Wu, L. Characterizing global marine heatwaves under a spatio-temporal framework. *Prog. Oceanogr.* **211**, 102947 (2023).

55. Scannell, H. A. et al. Spatiotemporal evolution of marine heatwaves globally. *ESS Open Archive* <https://doi.org/10.22541/essoar.169008275.57053412/v1> (July 23, 2023).

56. Perkins, S. E. & Alexander, L. V. On the measurement of heat waves. *J. Clim.* **26**, 4500–4517 (2013).

57. Frölicher, T. L., Fischer, E. M. & Gruber, N. Marine heatwaves under global warming. *Nature* **560**, 360–364 (2018).

58. Xu, T., Newman, M., Capotondi, A. & Di Lorenzo, E. The continuum of northeast Pacific marine heatwaves and their relationship to the Tropical Pacific. *Geophys. Res. Lett.* **48**, 2020GL090661 (2021).

59. Amaya, D. J., Miller, A. J., Xie, S.-P. & Kosaka, Y. Physical drivers of the summer 2019 North Pacific marine heatwave. *Nat. Commun.* **11**, 1903 (2020).

60. Cael, B. B., Burger, F. A., Henson, S. A., Britten, G. L. & Frölicher, T. L. Historical and future maximum sea surface temperatures. *Sci. Adv.* **10**, eadj5569 (2024).

61. Glynn, P. W. & D'Croz, L. Experimental evidence for high temperature stress as the cause of El Niño-coincident coral mortality. *Coral Reefs* **8**, 181–191 (1990).

62. Liu, G. et al. Reef-scale thermal stress monitoring of coral ecosystems: new 5-km global products from NOAA coral reef watch. *Remote Sens.* **6**, 11579–11606 (2014).

63. Langlais, C. E. et al. Coral bleaching pathways under the control of regional temperature variability. *Nat. Clim. Change* **7**, 839–844 (2017).

64. Kajtar, J. B. et al. A stakeholder-guided marine heatwave hazard index for fisheries and aquaculture. *Clim. Change* **177**, 26 (2024).

65. Oliver, E. C. J. et al. Longer and more frequent marine heatwaves over the past century. *Nat. Commun.* **9**, 1324 (2018).

66. Wulff, C. O., Vitart, F. & Domeisen, D. I. V. Influence of trends on subseasonal temperature prediction skill. *Q. J. R. Meteorol. Soc.* **148**, 1280–1299 (2022).

67. Jacox, M. G. Marine heatwaves in a changing climate. *Nature* **571**, 485–487 (2019).

68. Amaya, D. J. et al. Marine heatwaves need clear definitions so coastal community can adapt. *Nature* **616**, 29–32 (2023).

69. Mignot, A. et al. Decrease in air-sea CO₂ fluxes caused by persistent marine heatwaves. *Nat. Commun.* **13**, 4300 (2022).

70. Laufkötter, C., Zscheischler, J. & Frölicher, T. L. High-impact marine heatwaves attributable to human-induced global warming. *Science* **369**, 1621–1625 (2020).

71. Bonino, G., Masina, S., Galimberti, G. & Moretti, M. Southern Europe and western Asian marine heatwaves (SEWA-MHWs): a dataset based on macroevents. *Earth Syst. Sci. Data* **15**, 1269–1285 (2023).

72. Prochaska, J. X., Beaulieu, C. & Giamalaki, K. The rapid rise of severe marine heat wave systems. *Environ. Res. Clim.* **2**, 021002 (2023).

73. Desmet, F., Münnich, M. & Gruber, N. Spatiotemporal heterogeneity in the increase in ocean acidity extremes in the northeastern Pacific. *Biogeosciences* **20**, 5151–5175 (2023).

74. Donlon, C. J. et al. The Operational Sea Surface Temperature and Sea Ice Analysis (OSTIA) system. *Remote Sens. Environ.* **116**, 140–158 (2012).

75. Good, S. et al. The Current Configuration of the OSTIA system for operational production of foundation sea surface temperature and ice concentration analyses. *Remote Sens.* **12**, 720 (2020).

76. Huang, B. et al. Improvements of the Daily Optimum Interpolation Sea Surface Temperature (DOISST) Version 2.1. *J. Clim.* **34**, 2923–2939 (2021).

77. Cook, F. et al. Marine heatwaves in shallow coastal ecosystems are coupled with the atmosphere: Insights from half a century of daily in situ temperature records. *Front. Clim.* **4** <https://doi.org/10.3389/fclim.2022.1012022> (2022).

78. Goebeler, N., Norkko, A. & Norkko, J. Ninety years of coastal monitoring reveals baseline and extreme ocean temperatures are increasing off the Finnish coast. *Commun. Earth Environ.* **3**, 215 (2022).

79. Hemming, M., Roughan, M. & Schaeffer, A. Exploring multi-decadal time series of temperature extremes in Australian coastal waters. *Earth Syst. Sci. Data* **16**, 887–901 (2024).

80. Hu, S. et al. Observed strong subsurface marine heatwaves in the tropical western Pacific Ocean. *Environ. Res. Lett.* **16**, 104024 (2021).

81. Elzahaby, Y. & Schaeffer, A. Observational Insight Into the Subsurface Anomalies of Marine Heatwaves. *Front. Marine Sci.* **6** <https://doi.org/10.3389/fmars.2019.00745> (2019).

82. Johnson, G. C. et al. Argo—two decades: global oceanography, revolutionized. *Annu. Rev. Mar. Sci.* **14**, 379–403 (2022).

83. Bond, N. A., Cronin, M. F., Freeland, H. & Mantua, N. Causes and impacts of the 2014 warm anomaly in the NE Pacific. *Geophys. Res. Lett.* **42**, 3414–3420 (2015).

84. Capotondi, A., Sardeshmukh, P. D., Di Lorenzo, E., Subramanian, A. C. & Miller, A. J. Predictability of US West Coast Ocean Temperatures is not solely due to ENSO. *Sci. Rep.* **9**, 10993 (2019).

85. Jean-Michel, L. et al. The Copernicus Global 1/12° Oceanic and Sea Ice GLORYS12 Reanalysis. *Front. Earth Sci.* **9** <https://doi.org/10.3389/feart.2021.698876> (2021).

86. Amaya, D. J. et al. Bottom marine heatwaves along the continental shelves of North America. *Nat. Commun.* **14**, 1038 (2023).

87. Fredston, A. L. et al. Marine heatwaves are not a dominant driver of change in demersal fishes. *Nature* **621**, 324–329 (2023).

88. Carolina Castillo-Trujillo, A. et al. An evaluation of eight global ocean reanalyses for the Northeast U.S. Continental shelf. *Prog. Oceanogr.* **219**, 103126 (2023).

89. Penland, C. & Sardeshmukh, P. D. The optimal growth of tropical sea surface temperature anomalies. *J. Clim.* **8**, 1999–2024 (1995).

90. Sen Gupta, A. et al. Drivers and impacts of the most extreme marine heatwave events. *Sci. Rep.* **10**, 19359 (2020).

91. Perkins-Kirkpatrick, S. E. et al. The role of natural variability and anthropogenic climate change in the 2017/18 Tasman Sea Marine heatwave. *Bull. Am. Meteorol. Soc.* **100**, S105–S110 (2019).

92. Kajtar, J. B., Bachman, S. D., Holbrook, N. J. & Pilo, G. S. Drivers, dynamics, and persistence of the 2017/2018 Tasman Sea marine heatwave. *J. Geophys. Res. Oceans* **127**, e2022JC018931 (2022).

93. Salinger, M. J. et al. The unprecedented coupled ocean-atmosphere summer heatwave in the New Zealand region 2017/18: drivers, mechanisms and impacts. *Environ. Res. Lett.* **14**, 044023 (2019).

94. Gregory, C. H., Holbrook, N. J., Marshall, A. G. & Spillman, C. M. Atmospheric drivers of Tasman Sea marine heatwaves. *J. Clim.* **36**, 5197–5214 (2023).

95. Carrasco, D., Pizarro, O., Jacques-Coper, M. & Narváez, D. A. Main drivers of marine heat waves in the eastern South Pacific. *Front. Marine Sci.* **10** <https://doi.org/10.3389/fmars.2023.1129276> (2023).

96. Dasgupta, P., Nam, S., Saranya, J. S. & Roxy, M. K. Marine heatwaves in the East Asian marginal seas facilitated by boreal summer intraseasonal oscillations. *J. Geophys. Res. Oceans* **129**, e2023JC020602 (2024).

97. Amaya, D. J. et al. Are long-term changes in mixed layer depth influencing North Pacific marine heatwaves? *Bull. Am. Meteorol. Soc.* **102**, S59–S66 (2021).

98. Vogt, L., Burger, F. A., Griffies, S. M. & Frölicher, T. L. Local drivers of marine heatwaves: a global analysis with an earth system model. *Front. Clim.* **4** <https://doi.org/10.3389/fclim.2022.847995> (2022).

99. Feng, M., McPhaden, M. J., Xie, S.-P. & Hafner, J. La Niña forces unprecedented Leeuwin Current warming in 2011. *Sci. Rep.* **3**, 1277 (2013).

100. Benthuysen, J., Feng, M. & Zhong, L. Spatial patterns of warming off Western Australia during the 2011 Ningaloo Niño: Quantifying impacts of remote and local forcing. *Cont. Shelf Res.* **91**, 232–246 (2014).

101. Oliver, E. C. J. et al. The unprecedented 2015/16 Tasman Sea marine heatwave. *Nat. Commun.* **8**, 16101 (2017).

102. Li, Z., Holbrook, N. J., Zhang, X., Oliver, E. C. J. & Cougnon, E. A. Remote forcing of Tasman sea marine heatwaves. *J. Clim.* **33**, 5337–5354 (2020).

103. Elzahaby, Y., Schaeffer, A., Roughan, M. & Delaix, S. Oceanic circulation drives the deepest and longest marine heatwaves in the East Australian Current System. *Geophys. Res. Lett.* **48**, e2021GL094785 (2021).

104. Jin, F.-F. An equatorial ocean recharge paradigm for ENSO. Part I: conceptual model. *J. Atmos. Sci.* **54**, 811–829 (1997).

105. Capotondi, A. ENSO diversity in the NCAR CCSM4 climate model. *J. Geophys. Res. Oceans* **118**, 4755–4770 (2013).

106. Bian, C., Jing, Z., Wang, H. & Wu, L. Scale-dependent drivers of marine heatwaves globally. *Geophys. Res. Lett.* **51**, e2023GL107306 (2024).

107. Myers, T. A., Mechoso, C. R., Cesana, G. V., DeFlorio, M. J. & Waliser, D. E. Cloud feedback key to marine heatwave off Baja California. *Geophys. Res. Lett.* **45**, 4345–4352 (2018).

108. Schmeisser, L., Bond, N. A., Siedlecki, S. A. & Ackerman, T. P. The role of clouds and surface heat fluxes in the maintenance of the 2013–2016 Northeast Pacific marine heatwave. *J. Geophys. Res.: Atmos.* **124**, 10772–10783 (2019).

109. Mogen, S. C. et al. Multi-month forecasts of marine heatwaves and ocean acidification extremes. *Nat. Geosci.* (2024).

110. Capotondi, A. et al. Observational needs supporting marine ecosystems modeling and forecasting: from the global ocean to regional and coastal systems. *Front. Marine Sci.* **6** <https://doi.org/10.3389/fmars.2019.00623> (2019).

111. Ren, X., Liu, W., Capotondi, A., Amaya, D. J. & Holbrook, N. J. The Pacific Decadal Oscillation modulated marine heatwaves in the Northeast Pacific during past decades. *Commun. Earth Environ.* **4**, 218 (2023).

112. Wang, Y., Holbrook, N. J. & Kajtar, J. B. Predictability of marine heatwaves off western Australia using a linear inverse model. *J. Clim.* **36**, 6177–6193 (2023).

113. Wang, C. Three-ocean interactions and climate variability: a review and perspective. *Clim. Dyn.* **53**, 5119–5136 (2019).

114. Cai, W. et al. Pantropical climate interactions. *Science* **363**, eaav4236 (2019).

115. Yao, Y., Wang, C. & Wang, C. Record-breaking 2020 summer marine heatwaves in the western North Pacific. *Deep Sea Res. Part II Top. Stud. Oceanogr.* **209**, 105288 (2023).

116. Song, Q., Yao, Y. & Wang, C. Response of future summer marine heatwaves in the South China Sea to enhanced Western Pacific subtropical high. *Geophys. Res. Lett.* **50**, e2023GL103667 (2023).

117. Song, Q., Wang, C., Yao, Y. & Fan, H. Unraveling the Indian monsoon's role in fueling the unprecedented 2022 Marine Heatwave in the Western North Pacific. *npj Clim. Atmos. Sci.* **7**, 90 (2024).

118. Chiang, J. C. H. & Vimont, D. J. Analogous Pacific and Atlantic meridional modes of tropical atmosphere–ocean variability. *J. Clim.* **17**, 4143–4158 (2004).

119. Zhang, H., Clement, A. & Di Nezio, P. The South Pacific meridional mode: a mechanism for ENSO-like variability. *J. Clim.* **27**, 769–783 (2014).

120. Gregory, C. H., Holbrook, N. J., Marshall, A. G. & Spillman, C. M. Sub-seasonal to seasonal drivers of regional marine heatwaves around Australia. *Clim. Dyn.* <https://doi.org/10.1007/s00382-024-07226-x> (2024).

121. Köhn, E. E., Vogt, M., Münnich, M. & Gruber, N. On the vertical structure and propagation of marine heatwaves in the Eastern Pacific. *J. Geophys. Res. Oceans* **129**, e2023JC020063 (2024).

122. Alexander, M. A., Deser, C. & Timlin, M. S. The reemergence of SST anomalies in the North Pacific Ocean. *J. Clim.* **12**, 2419–2433 (1999).

123. Scannell, H. A., Johnson, G. C., Thompson, L., Lyman, J. M. & Riser, S. C. Subsurface evolution and persistence of marine heatwaves in the Northeast Pacific. *Geophys. Res. Lett.* **47**, e2020GL090548 (2020).

124. Richaud, B. et al. Drivers of marine heatwaves in the Arctic Ocean. *J. Geophys. Res. Oceans* **129**, e2023JC020324 (2024).

125. Zscheischler, J. et al. Future climate risk from compound events. *Nat. Clim. Change* **8**, 469–477 (2018).

126. Seneviratne, S. I. et al. in *Climate Change 2021: The Physical Science Basis. Contribution of Working Group I to the Sixth Assessment Report of the Intergovernmental Panel on Climate Change* (eds V. Masson-Delmotte et al.) Ch. Weather and Climate Extreme Events in a Changing Climate, 1513–1766 (Cambridge University Press, 2021).

127. Peng, Q., Xie, S.-P., Wang, D., Zheng, X.-T. & Zhang, H. Coupled ocean-atmosphere dynamics of the 2017 extreme coastal El Niño. *Nat. Commun.* **10**, 298 (2019).

128. Hauri, C., Gruber, N., McDonnell, A. M. P. & Vogt, M. The intensity, duration, and severity of low aragonite saturation state events on the California continental shelf. *Geophys. Res. Lett.* **40**, 3424–3428 (2013).

129. Negrete-García, G., Lovenduski, N. S., Hauri, C., Krumhardt, K. M. & Lauvset, S. K. Sudden emergence of a shallow aragonite saturation horizon in the Southern Ocean. *Nat. Clim. Change* **9**, 313–317 (2019).

130. Burger, F. A., John, J. G. & Frölicher, T. L. Increase in ocean acidity variability and extremes under increasing atmospheric CO₂. *Biogeosciences* **17**, 4633–4662 (2020).

131. Burger, F. A. & Frölicher, T. L. Drivers of surface ocean acidity extremes in an earth system model. *Glob. Biogeochem. Cycles* **37**, e2023GB007785 (2023).

132. Köhn, E. E., Münnich, M., Vogt, M., Desmet, F. & Gruber, N. Strong habitat compression by extreme shoaling events of hypoxic waters in the Eastern Pacific. *J. Geophys. Res.: Oceans* **127**, e2022JC018429 (2022).

133. Le Grix, N., Zscheischler, J., Laufkötter, C., Rousseaux, C. S. & Frölicher, T. L. Compound high-temperature and low-chlorophyll extremes in the ocean over the satellite period. *Biogeosciences* **18**, 2119–2137 (2021).

134. Le Grix, N., Zscheischler, J., Rodgers, K. B., Yamaguchi, R. & Frölicher, T. L. Hotspots and drivers of compound marine heatwaves and low net primary production extremes. *Biogeosciences* **19**, 5807–5835 (2022).

135. Boyd, P. W. & Brown, C. J. Modes of interactions between environmental drivers and marine biota. *Front. Marine Sci.* **2** (2015).

136. Pörtner, H. O. & Knust, R. Climate change affects marine fishes through the oxygen limitation of thermal tolerance. *Science* **315**, 95–97 (2007).

137. Deutsch, C., Ferrel, A., Seibel, B., Pörtner, H.-O. & Huey, R. B. Climate change tightens a metabolic constraint on marine habitats. *Science* **348**, 1132–1135 (2015).

138. Morée, A. L., Clarke, T. M., Cheung, W. W. L. & Frölicher, T. L. Impact of deoxygenation and warming on global marine species in the 21st century. *EGUsphere* **2022**, 1–36 (2022).

139. Bednaršek, N. et al. Natural analogues in pH variability and predictability across the Coastal Pacific estuaries: extrapolation of the increased oyster dissolution under increased pH amplitude and low predictability related to ocean acidification. *Environ. Sci. Technol.* **56**, 9015–9028 (2022).

140. Hoegh-Guldberg, O. et al. Coral Reefs under rapid climate change and ocean acidification. *Science* **318**, 1737–1742 (2007).

141. Le Grix, N., Cheung, W. L., Reygondeau, G., Zscheischler, J. & Frölicher, T. L. Extreme and compound ocean events are key drivers of projected low pelagic fish biomass. *Glob. Change Biol.* **29**, 6478–6492 (2023).

142. Cavole, L. M. et al. Biological Impacts of the 2013–2015 warm-water Anomaly in the Northeast Pacific Winners, losers, and the future. *Oceanography* **29**, 273–285 (2016).

143. Burger, F. A., Terhaar, J. & Frölicher, T. L. Compound marine heatwaves and ocean acidity extremes. *Nat. Commun.* **13**, 4722 (2022).

144. Wyatt, A. M., Resplandy, L. & Marchetti, A. Ecosystem impacts of marine heat waves in the northeast Pacific. *Biogeosciences* **19**, 5689–5705 (2022).

145. Mogen, S. C. et al. Ocean biogeochemical signatures of the North Pacific Blob. *Geophys. Res. Lett.* **49**, e2021GL096938 (2022).

146. Frölicher, T. L., Rodgers, K. B., Stock, C. A. & Cheung, W. W. L. Sources of uncertainties in 21st century projections of potential ocean ecosystem stressors. *Glob. Biogeochem Cycles* **30**, 1224–1243 (2016).

147. Kwiatkowski, L. et al. Twenty-first century ocean warming, acidification, deoxygenation, and upper-ocean nutrient and primary production decline from CMIP6 model projections. *Biogeosciences* **17**, 3439–3470 (2020).

148. Kwiatkowski, L. & Orr, J. C. Diverging seasonal extremes for ocean acidification during the twenty-first century. *Nat. Clim. Change* **8**, 141–145 (2018).

149. Kwiatkowski, L., Torres, O., Aumont, O. & Orr, J. C. Modified future diurnal variability of the global surface ocean CO₂ system. *Glob. Change Biol.* **29**, 982–997 (2023).

150. Qiu, Z., Qiao, F., Jang, C. J., Zhang, L. & Song, Z. Evaluation and projection of global marine heatwaves based on CMIP6 models. *Deep Sea Res. Part II Top. Stud. Oceanogr.* **194**, 104998 (2021).

151. Deser, C. et al. Insights from Earth system model initial-condition large ensembles and future prospects. *Nat. Clim. Change* **10**, 277–286 (2020).

152. Alexander, M. A. et al. Projected sea surface temperatures over the 21st century: Changes in the mean, variability and extremes for large marine ecosystem regions of Northern Oceans. *Elementa Sci. Anthropocene* **6** <https://doi.org/10.1525/elementa.191> (2018).

153. McAdam, R., Masina, S. & Gualdi, S. Seasonal forecasting of subsurface marine heatwaves. *Commun. Earth Environ.* **4**, 225 (2023).

154. de Boisseson, E. & Balmaseda, M. Predictability of Marine Heatwaves: assessment based on the ECMWF seasonal forecast system. *EGUsphere* **2023**, 1–19 (2023).

155. Hu, Z.-Z., Kumar, A., Jha, B., Zhu, J. & Huang, B. Persistence and predictions of the remarkable warm anomaly in the Northeastern Pacific Ocean during 2014–16. *J. Clim.* **30**, 689–702 (2017).

156. Amaya, D. J., Bond, N. A., Miller, A. J. & De Florio, M. J. The evolution and known atmospheric forcing mechanisms behind the 2013–2015 North Pacific warm anomalies. *US CLIVAR Variations* **14** (2016).

157. Wang, Y., Kajtar, J. B., Alexander, L. V., Pilo, G. S. & Holbrook, N. J. Understanding the changing nature of marine cold-spells. *Geophys. Res. Lett.* **49**, e2021GL097002 (2022).

158. Park, J.-Y., Stock, C. A., Dunne, J. P., Yang, X. & Rosati, A. Seasonal to multiannual marine ecosystem prediction with a global Earth system model. *Science* **365**, 284–288 (2019).

159. Frölicher, T. L., Ramseyer, L., Raible, C. C., Rodgers, K. B. & Dunne, J. Potential predictability of marine ecosystem drivers. *Biogeosciences* **17**, 2061–2083 (2020).

160. Mogen, S. C. et al. Skillful multi-month predictions of ecosystem stressors in the surface and subsurface ocean. *Earth's Future* **11**, e2023EF003605 (2023).

161. Forster, P. M. et al. Indicators of Global Climate Change 2023: annual update of key indicators of the state of the climate system and human influence. *Earth Syst. Sci. Data* **16**, 2625–2658 (2024).

162. Yao, Y., Wang, C. & Fu, Y. Global marine heatwaves and cold-spells in present climate to future projections. *Earth's Future* **10**, e2022EF002787 (2022).

163. Frankignoul, C., Gastineau, G. & Kwon, Y.-O. Estimation of the SST response to anthropogenic and external forcing and its impact on the Atlantic Multidecadal Oscillation and the Pacific Decadal Oscillation. *J. Clim.* **30**, 9871–9895 (2017).

164. Wills, R. C. J., Battisti, D. S., Armour, K. C., Schneider, T. & Deser, C. Pattern recognition methods to separate forced responses from internal variability in climate model ensembles and observations. *J. Clim.* **33**, 8693–8719 (2020).

165. Capotondi, A., Alexander, M. A., Bond, N. A., Curchitser, E. N. & Scott, J. D. Enhanced upper ocean stratification with climate change in the CMIP3 models. *J. Geophys. Res. Oceans* **117** <https://doi.org/10.1029/2011JC007409> (2012).

166. Cai, W. et al. Changing El Niño–Southern Oscillation in a warming climate. *Nat. Rev. Earth Environ.* **2**, 628–644 (2021).

167. Geng, T., Yang, Y. & Wu, L. On the mechanisms of Pacific Decadal Oscillation modulation in a warming climate. *J. Clim.* **32**, 1443–1459 (2019).

168. O'Brien, J. P. & Deser, C. Quantifying and understanding forced changes to unforced modes of atmospheric circulation variability over the North Pacific in a coupled model large ensemble. *J. Clim.* **36**, 19–37 (2023).

169. Song, S.-Y., Yeh, S.-W., Kim, H. & Holbrook, N. J. Arctic warming contributes to increase in Northeast Pacific marine heatwave days over the past decades. *Commun. Earth Environ.* **4**, 25 (2023).

170. Maher, N. et al. The future of the El Niño–Southern Oscillation: using large ensembles to illuminate time-varying responses and inter-model differences. *Earth Syst. Dyn.* **14**, 413–431 (2023).

171. Zhao, Y. & Yu, J.-Y. Two Marine Heatwave (MHW) variants under a basinwide MHW conditioning mode in the North Pacific and their Atlantic Associations. *J. Clim.* **36**, 8657–8674 (2023).

172. Shi, J. et al. Northeast Pacific warm blobs sustained via extratropical atmospheric teleconnections. *Nat. Commun.* **15**, 2832 (2024).

173. Ross, A. C. et al. A high-resolution physical–biogeochemical model for marine resource applications in the northwest Atlantic (MOM6-COBALT-NWA12 v1.0). *Geosci. Model Dev.* **16**, 6943–6985 (2023).

174. Cheeseman, T. et al. Bellwethers of change: population modelling of North Pacific humpback whales from 2002 through 2021 reveals shift from recovery to climate response. *R. Soc. Open Sci.* **11** <https://doi.org/10.1098/rsos.231462> (2024).

175. Huang, B. et al. Extended reconstructed sea surface temperature, version 5 (ERSSTv5): upgrades, validations, and intercomparisons. *J. Clim.* **30**, 8179–8205 (2017).

176. Watson, G. & Rousseaux, C. S. NASA Ocean Biogeochemical Model assimilating satellite chlorophyll global data daily VR2017, Goddard Earth Sciences Data and Information Services Center (GES DISC), Greenbelt, MD, USA, <https://doi.org/10.5067/PT6TXZKSHBW9> (2017).

177. Kirtman, B. P. et al. The North American multimodel ensemble: phase-1 seasonal-to-interannual prediction; Phase-2 toward developing intraseasonal prediction. *Bull. Am. Meteorol. Soc.* **95**, 585–601 (2014).

178. Ripple, W. J. et al. The 2023 state of the climate report: entering uncharted territory. *BioScience* **73**, 841–850 (2023).

179. Kuhlbrodt, T., Swaminathan, R., Ceppli, P. & Wilder, T. A glimpse into the future: the 2023 ocean temperature and sea ice extremes in the context of longer-term climate change. *Bull. Am. Meteorol. Soc.* **105**, E474–E485 (2024).

180. Cheng, L. et al. New record ocean temperatures and related climate indicators in 2023. *Adv. Atmos. Sci.* <https://doi.org/10.1007/s00376-024-3378-5> (2024).

181. Ceppli, P. & Fueglistaler, S. The El Niño–southern oscillation pattern effect. *Geophys. Res. Lett.* **48**, e2021GL095261 (2021).

182. Zhang, W., Jiang, F., Stuecker, M. F., Jin, F.-F. & Timmermann, A. Spurious North Tropical Atlantic precursors to El Niño. *Nat. Commun.* **12**, 3096 (2021).

183. Deser, C., Alexander, M. A., Xie, S.-P. & Phillips, A. S. Sea surface temperature variability: patterns and mechanisms. *Annu. Rev. Mar. Sci.* **2**, 115–143 (2010).

184. Diamond, M. S. Detection of large-scale cloud microphysical changes within a major shipping corridor after implementation of the International Maritime Organization 2020 fuel sulfur regulations. *Atmos. Chem. Phys.* **23**, 8259–8269 (2023).

185. Schoeberl, M. R. et al. The estimated climate impact of the Hunga Tonga-Hunga Ha'apai Eruption Plume. *Geophys. Res. Lett.* **50**, e2023GL104634 (2023).

186. Benthuysen, J. A., Oliver, E. C. J., Feng, M. & Marshall, A. G. Extreme marine warming across tropical Australia during austral summer 2015–2016. *J. Geophys. Res. Oceans* **123**, 1301–1326 (2018).

187. Benthuysen, J. A., Steinberg, C., Spillman, C. M. & Smith, G. A. Oceanographic drivers of bleaching in the GBR: from observations to prediction. Volume 4: Observations and predictions of marine heatwaves. *Report to the National Environmental Science Program. Reef and Rainforest Research Centre Limited*, Cairns (47pp). Accessed from: https://nesptropical.edu.au/wp-content/uploads/2021/2006/2024.2022-Volume-2024-Final-Report_COMPLETE.pdf (2021).

188. Benthuysen, J. A., Smith, G. A., Spillman, C. M. & Steinberg, C. R. Subseasonal prediction of the 2020 Great Barrier Reef and Coral Sea marine heatwave. *Environ. Res. Lett.* **16**, 124050 (2021).

189. Govekar, P. D., Griffin, C. & Beggs, H. Multi-sensor sea surface temperature products from the Australian Bureau of Meteorology. *Remote Sens.* **14**, 3785 (2022).

190. IMOS2024a. IMOS 6-day Night-time Multi-Sensor L3S gridded multiple-sensor multiple-swath Australian region skin SST (L3SM-6d). <https://portal.aodn.org.au/search?uuid=e1908591-b3cf-42aa-a32f-424322b28165>. Accessed 17 March 2024.

191. Wijffels, S. E. et al. A fine spatial-scale sea surface temperature atlas of the Australian regional seas (SSTAARS): Seasonal variability and trends around Australasia and New Zealand revisited. *J. Mar. Syst.* **187**, 156–196 (2018).

192. IMOS2024b. Sensors on Tropical Research Vessels: Enhanced Measurements from Ships of Opportunity (SOOP). <https://portal.aodn.org.au/search?uuid=8af21108-c535-43bf-8dab-c1f45a26088c>. Accessed 22 March 2024.

193. Argo2020. Argo float data and metadata from Global Data Assembly Centre (Argo GDAC) - Snapshot of Argo GDAC of February 10st 2020. SEANOE. <https://doi.org/10.17882/42182#70590>.

194. IMOS2024c. IMOS – Argo Profiles – core data. <https://portal.aodn.org.au/search?uuid=4402cb50-e20a-44ee-93e6-4728259250d2>. Accessed 26 March 2024.

195. Ridgway, K. R., Dunn, J. R. & Wilkin, J. L. Ocean interpolation by four-dimensional weighted least squares—application to the waters around Australasia. *J. Atmos. Ocean. Technol.* **19**, 1357–1375 (2002).

196. IMOS2024d. IMOS - Australian National Facility for Ocean Gliders (ANFOG) - delayed mode glider deployments. <https://portal.aodn.org.au/search?uuid=c317b0fe-02e8-4ff9-96c9-563fd58e82ac>. Accessed 18 March 2024.

197. IMOS2024e. IMOS - ANMN National Reference Stations - Darwin and Yongala - Near real-time meteorology and oceanographical data. <https://portal.aodn.org.au/search?uuid=006bb7dc-860b-4b89-bf4c-6bd930bd35b7>. Accessed 17 March 2024.

198. IMOS2024f. IMOS NRS. IMOS - Australian National Mooring Network (ANMN) Facility - WQM and CTD burst averaged data products. <https://portal.aodn.org.au/search?uuid=8964658c-6ee1-4015-9bae-2937dfcc6ab9>. Accessed 19 March 2024.

199. AIMS2009. Northern Australia Automated Marine Weather and Oceanographic Stations. <https://doi.org/10.25845/5c09bf93f315d>. Accessed 17 March 2024.

200. AIMS2017. AIMS Sea Water Temperature Observing System (AIMS Temperature Logger Program). <https://doi.org/10.25845/5b4eb0f9bb848>. Accessed 28 November 2023.

Acknowledgements

This paper is a product of the CLIVAR “Marine Heatwaves in the Global Ocean” Research Focus Group. The authors thank CLIVAR for their sponsorship and the CLIVAR Program Office for their support. AC was supported by the NOAA Climate Program Office’s CVP and MAPP programs, DOE Award #DE-SC0023228, and NASA Physical Oceanography grant #80NSSC21K0556. ASG was supported by an Australian Research Council Future Fellowship (FT220100475). NSL was supported by U.S. National Science Foundation (OCE-1752724) and the NOAA CVP program (NA20OAR4310405). CM acknowledges support from Proyecto ANID Fondecyt código 3200621, and Data Observatory Foundation ANID Technology Center No. DO210001. CW acknowledges funding from the National Key R&D Program of China (2019YFA0606701) and National Natural Science Foundation of China (42192564). TLF acknowledges funding from AtlantECO (project number: 862923) as well as TipESM, which are both funded by the European Union. Views and opinions expressed are however those of the author(s) only and do not necessarily reflect those of the European Union or the European Climate, Infrastructure and Environment Executive Agency (CINEA). Neither the European Union nor the granting authority can be held responsible for them. NJH acknowledges support from the ARC Center of Excellence for Climate Extremes (CE170100023) and the National Environmental Science Program Climate Systems Hub. NCAR is sponsored by the National Science Foundation under Cooperative Agreement 1852977. We thank Adam S. Phillips (NCAR) for helping with the preparation of Figs. 4 and 6, and Dr. Michael Jacox (NOAA) for his assistance with the data used to prepare Fig. 5. Argo data were collected and made freely available by the International Argo Program and the national programs that contribute to it. (<https://argo.ucsd.edu>, <https://www.ocean-ops.org>). The Argo Program is part of the Global Ocean Observing System. Data was sourced from Australia’s Integrated Marine Observing System (IMOS) - IMOS is enabled by the National Collaborative Research Infrastructure Strategy (NCRIS).

Author contributions

Antonietta Capotondi: conceptualization, writing – original draft, writing - review and editing, visualization. Regina R. Rodrigues: conceptualization,

writing – original draft. Alex Sen Gupta: writing – original draft, writing- review and editing, visualization. Jessica A. Benthuysen: writing – original draft, writing - review and editing, visualization. Clara Deser: writing – original draft, visualization. Thomas L. Frölicher: writing – original draft, visualization. Nicole S. Lovenduski: writing – original draft, visualization. Dillon J. Amaya: writing – original draft, visualization. Natacha Le Grix: writing - review and editing, visualization. Tongtong Xu: writing - review and editing, visualization. Juliet Hermes: writing - review and editing. Neil J. Holbrook: writing – original draft. Cristian Martinez-Villalobos: writing – original draft. Simona Masina: writing - review and editing. Mathew Koll Roxy: writing – original draft. Amandine Schaeffer: writing - review and editing. Robert W. Schlegel: writing - review and editing. Kathryn E. Smith: writing – original draft. Chunzai Wang: writing - review and editing.

Competing interests

The authors declare no competing interests. Prof. Regina Rodrigues is an Editorial Board Member for *Communications Earth & Environment*, but was not involved in the editorial review of, nor the decision to publish this article.

Additional information

Supplementary information The online version contains supplementary material available at <https://doi.org/10.1038/s43247-024-01806-9>.

Correspondence and requests for materials should be addressed to Antonietta Capotondi.

Peer review information *Communications Earth & Environment* thanks the anonymous reviewers for their contribution to the peer review of this work. Primary Handling Editor: Alireza Bahadori. A peer review file is available

Reprints and permissions information is available at <http://www.nature.com/reprints>

Publisher’s note Springer Nature remains neutral with regard to jurisdictional claims in published maps and institutional affiliations.

Open Access This article is licensed under a Creative Commons Attribution 4.0 International License, which permits use, sharing, adaptation, distribution and reproduction in any medium or format, as long as you give appropriate credit to the original author(s) and the source, provide a link to the Creative Commons licence, and indicate if changes were made. The images or other third party material in this article are included in the article’s Creative Commons licence, unless indicated otherwise in a credit line to the material. If material is not included in the article’s Creative Commons licence and your intended use is not permitted by statutory regulation or exceeds the permitted use, you will need to obtain permission directly from the copyright holder. To view a copy of this licence, visit <http://creativecommons.org/licenses/by/4.0/>.

© The Author(s) 2024

¹Cooperative Institute for Research in Environmental Sciences, University of Colorado Boulder, Boulder, CO, USA. ²NOAA/Physical Sciences Laboratory, Boulder, CO, USA. ³Federal University of Santa Catarina, Florianópolis, Brazil. ⁴Climate Change Research Centre and Centre for Marine Science and Innovation, University of New South Wales, Sydney, NSW, Australia. ⁵Australian Research Council, Centre of Excellence for Climate Extremes, University of New South Wales, Sydney, NSW, Australia. ⁶Australian Institute of Marine Science, Crawley, WA, Australia. ⁷Climate and Global Dynamics Laboratory, National Center for Atmospheric Research, Boulder, CO, USA. ⁸Climate and Environmental Physics, Physics Institute, University of Bern, Bern, Switzerland. ⁹Oeschger Centre for Climate Change Research, University of Bern, Bern, Switzerland. ¹⁰Department of Atmospheric and Oceanic Sciences and Institute of Arctic and Alpine Research, University of Colorado Boulder, Boulder, CO, USA. ¹¹South African Environmental Observation Network, Cape Town, South Africa. ¹²Institute for Marine and Antarctic Studies, University of Tasmania,

Hobart, TAS, Australia. ¹³ARC Centre of Excellence for Climate Extremes, University of Tasmania, Hobart, TAS, Australia. ¹⁴Faculty of Engineering and Science, Universidad Adolfo Ibáñez, Santiago, Chile. ¹⁵Data Observatory Foundation, ANID Technology Center No. DO210001, Santiago, Chile. ¹⁶CMCC Foundation—Euro-Mediterranean Center on Climate Change, Bologna, Italy. ¹⁷Centre for Climate Change Research, Indian Institute of Tropical Meteorology, Ministry of Earth Sciences, Pune, India. ¹⁸School of Mathematics and Statistics, UNSW, Sydney, NSW, Australia. ¹⁹Center for Marine Science and Innovation, UNSW, Sydney, NSW, Australia. ²⁰Laboratoire d'Océanographie de Villefranche, Sorbonne University, CNRS, Villefranche-sur-mer, France. ²¹Marine Biological Association of the United Kingdom, Plymouth, UK. ²²State Key Laboratory of Tropical Oceanography, South China Sea Institute of Oceanology, Chinese Academy of Sciences, Guangzhou, China. ²³Global Ocean and Climate Research Center, South China Sea Institute of Oceanology, Chinese Academy of Sciences, Guangzhou, China. ²⁴Guangdong Key Laboratory of Ocean Remote Sensing, South China Sea Institute of Oceanology, Chinese Academy of Sciences, Guangzhou, China.

✉ e-mail: antonietta.capotondi@noaa.gov